Fall 2020
Volume 19
Issue 1

UNIVERSITY of ROCHESTER

"THERE ARE NO SMALL JOBS AT SSP"

Vice Admiral Johnny R. Wolfe, Jr.
Director, Strategic Systems Programs

If interested send resumes to: SSPrecruitment@ssp.navy.mil

Journal of Undergraduate Research

Volume Nineteen, Issue One

Fall 2020

UNIVERSITY of ROCHESTER

The Journal of Undergraduate Research (JUR) is dedicated to providing the student body with intellectual perspectives from various academic disciplines. JUR serves as a forum for the presentation of original research, thereby encouraging the pursuit of significant scholarly endeavors.

Journal Staff

Editors-in-Chief

John Roy Lozada '21
Shelby Sabourin '21

Managing Editors

Katya Mueller '21
Emily Lainoff '21
Hannah Jaques '21
Nisha Arya '22

Business Manager

Jobi Jose '22

Website Editor

Shina Park '23

Layout & Design Chair

Oion Akif '21

Content Editors

Erin Bevec '23
Brent Lee '24
Jocelyn Mathew '23
Ian Poe '24

Layout Editors

Oion Akif '21
Brighid Bugos
Shina Park '23

Cover Design

Oion Akif

Acknowledgements

Director of Undergraduate Research

Dr. Sina Ghaemmaghami

Dean of the College

Dr. Jeffrey Runner

Review Board

Dan Alexander
Tanya Bakhmetyeva
Janet Berlo
John Criswell
Kevin Davis
Chen Ding
Julie Fudge
Sarah Higley
Robert Jacobs
Chigusa Kurumada
Kenwin Maung
Sarah McConnell
Renee Miller
Steven Rozenski
Brianna Theobald
Martin Yang
Nese Yildiz

Journal of Undergraduate Research

University of Rochester • Volume 19, Issue 1 • Fall 2020

This issue of the Journal of Undergraduate Research was assembled on macOS Big Sur using Affinity Publisher. Microsoft Word and Google Docs were used for text editing and review. Fonts used include Minion Pro, the main font for body text, and Myriad Pro, the main font for headings and decorative text. This physical version of this journal was bound by Emerald Print Management of Rochester, NY.

Represent Rochester.

Join JUR.

Interested in publishing in our upcoming issues?
*Submit your paper to us at **jurrochester.com**.*

Letter from the Editors

With the release of our Fall 2020 edition of the University of Rochester's Journal of Undergraduate Research, we mark approximately one year since our new "normal" began. In the passing year, we all have faced many unexpected challenges and difficulties, both personal and professional. Nonetheless, we pushed forward - we adapted to the new social climate and adjusted to the "Zoom" life. While we hope to return to the joys of in-person interactions in the near future, we must celebrate our triumphs in the last year and embrace the profound changes COVID-19 has brought upon the academic community. This pandemic has highlighted the tremendous value of research and scholarship, as well as the benefits they bring forth to society.

In this edition of JUR, we present four articles from our fellow undergraduate students that highlight the level of scholarship present on campus. With these articles ranging from linguistics to chemistry, we hope to demonstrate that research can be done in any field. In doing so, we hope to encourage our readers to pursue their own scholarly activities in whatever subject sparks their curiosity. Speaking from personal experience, research has truly paved our academic careers and contributed greatly to our time at the University of Rochester where research is a hallmark of the campus community. We hope that such pursuits may have a similar positive impact for you as it has for us.

To all of our authors, faculty, and editorial team, we are extremely grateful for your contributions that help JUR achieve our mission of showcasing the research done on campus. We could not do this without all of your help.

To our readers, we hope you enjoy reading the Fall 2020 edition of JUR and look forward to seeing your own works in the future.

Sincerely,

John Roy Lozada & Shelby Sabourin

Editors-in-Chief

Investigating the Phase Behavior of Bead-Spring Polymer Blends With Molecular Dynamics Simulations

Oion Akif '21, *Chemical Engineering*

Advised by Heta Gandhi & Andrew White, *Department of Chemical Engineering*

Introduction

Phase diagrams of polymer mixtures are useful in a myriad of areas, including applications in industry,[1,2,3,4] materials science research,[5,6] as well as many other scientific applications.[7,8] Use of such diagrams enable better prediction of experimental outcomes.[9] If a particular phase is desired for a material such as a paint, coating, or ink due to its desirable properties, a phase diagram can assist in providing valuable information about the most feasible conditions it exists in, which can allow for more efficient augmentation of experiments for its creation.

Interactions between unlike molecules are a driving force in the creation of observed phases of blends.[1] An interaction parameter related to the strength of interactions between molecules of the polymer was created, as defined in greater detail in a later section. This served as a quantitative measure of the relative interaction between the two monomers simulated. Two distinct systems of binary polymer blends were simulated to investigate their phase behavior with changing temperature and interaction coefficient.

A *polymer* is a repeating chain of similar molecules, each known as a monomer, that are chemically bonded to each other. The number of monomers comprising a polymer is known as the polymer's degree of polymerization.[10]

There are an almost endless possible combinations of monomers, which can create a vast range of polymer structures. Polymers may be divided into various different classes depending on how the different monomers are arranged. One classification is through differing connectivity, and are called the linear, branched-chain, and network polymers.[10,11] As the names suggest, a linear polymer consists of monomers connected to each other in a single linear chain, whereas in a branched-chain polymer branches are allowed from the main chain. A network polymer may have branches connected to other branches to produce highly complicated structures.[12] In this study, we are only concerned with the simplest class, linear polymers, as phase behavior of the more complex macromolecules are not yet well-understood.[1]

Linear polymers can be further classified as linear homopolymers that comprise of only one type of monomers and copolymers that constitutes multiple types of monomers.[10] A block copolymer is a polymer made of smaller blocks of polymers, which contain the same monomer, connected to each other.[13] If a block copolymer contains two blocks of different types, it is known as a diblock copolymer.[10] For simplicity, we have only considered mixtures of linear homopolymers and diblock copolymers in our study.

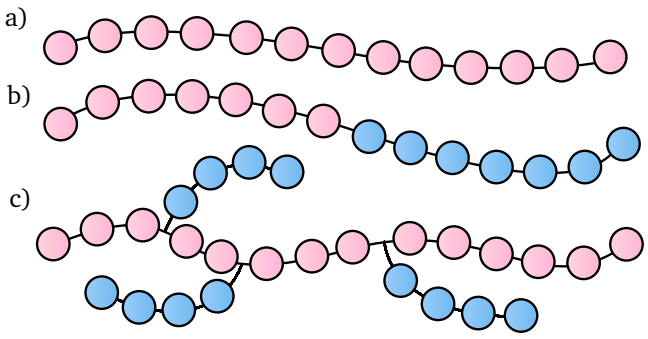

Figure 1. *Different types of polymers, where each color represents a different monomer. The polymers represented are the a) linear homopolymer, b) (linear) diblock copolymer, and c) a branched chain copolymer.*

A *phase* is traditionally described as a mechanically separable part of a system that either can itself (or contains a constituent which can) become part of another state in a reversible way.[14] However, in the context of polymer mixtures, phases can be defined based on the microstructures that they form.[1,15] A phase diagram gives information about the phase of a system under a set of thermodynamic conditions in an easily visualized graphic. The thermodynamic conditions or phase space to be investigated can be chosen and are typically placed on the diagram's axes. In this study, the phase behavior of mixtures will be studied by varying temperature and interaction parameter, creating a 2-dimensional phase diagram. The interaction parameter will be discussed in more detail in a further section.

The phase behavior of two polymer blends—the homopolymer-homopolymer and the homopolymer-diblock copolymer blends—were investigated, as both of these have been widely researched in literature due to their being the simplest polymer architectures of the polymer and block copolymers respectively.[1,16,17,18,19,20]

Methods

Initial System Configuration

The systems were initialized in ordered arrays of polymers all parallel to each other. The first system (homopolymer blend) was comprised of one linear homopolymer with beads of type A, and one homopolymer with beads of type B, as shown in

Figure 2a, alternating next to each other. Each homopolymer had a degree of polymerization of 40. The dimensions of this array was $20 \times 20 \times 1$, which created a prism-like box. This system contained $N = 16{,}000$ beads in 400 polymers.

The second system (diblock polymer blend) consisted of two linear homopolymers (of types A and B respectively), and one diblock polymer with equal-sized A and B blocks. Each polymer had a degree of polymerization of 40. The three polymers were initialized next to each other as shown in Figure 2b in a $24 \times 24 \times 1$ array. This system contained $N = 23{,}040$ beads in 576 polymers.

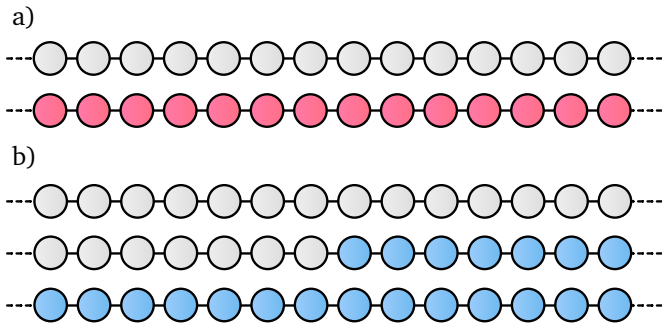

Figure 2. *Initial configuation of the polymer blends, where a) is the linear homopolymer mixture system and b) is the linear homopolymer-diblock copolymer system. White, red, and blue beads represent three different types of beads.*

Molecular Dynamics

In a real system at the molecular level, each particle will experience a force by all other particles in the system.[21] This force may be attractive or repulsive, and is generally a function of the distance between the particles. Most atoms will experience a strong repulsive force if they come too close to each other, but experience an attractive force otherwise, which decreases in magnitude with increasing separation.[22,23] Given an initial ensemble of particles with well-defined positions, the net force on a particle may be calculated by taking the vector sum of the forces it experiences due to all of the other particles in the ensemble. We can repeat this for all particles to determine all the forces at some time t.

With this information, we can calculate the distance the particles move during some small timestep Δt using Newton's laws of motion.[24] A rough idea about how this is calculated can be seen in Newton's second law of motion, which can relate the force on a body to the distance it travels:[25]

$$F = ma = \frac{\mathrm{d}^2 x}{\mathrm{d}t^2}. \tag{1}$$

This allows us to find the new position of the particles at time $t + \Delta t$. The calculation is performed by the simulation engine using an *integrator*, which uses numerical methods for integrating the equations of motion.[26] Since the particle positions have changed, the forces on them have changed as well and must be recalculated, and the procedure is repeated for a large number of timesteps. The resulting path the particles follow is stored in a "trajectory" file by the simulation software.

Forces on a particle are not generally determined directly. Instead, the force acting on a particle because of another particle is calculated from the potential energy between the two particles. If a pair of particles has a negative potential, the particles will experience an equal and opposite attractive force on each other—much like the gravitational force pulling a pair of celestial bodies together. A positive potential implies the particles will experience a repulsive force between themselves. From this so-called "pair potential" the direction and magnitude of the force can be determined. By determining the potentials between each particle pair in the system, the total force on each particle can be calculated.

This simulation method is known as molecular dynamics (MD), which aims to emulate the natural motion of particles in a system.[27] MD can be performed very efficiently by molecular dynamics software such as HOOMD-blue.[22,23]

The accuracy of this method largely depends on the how well the potentials between particles can be modeled. Although no simulation models the forces on the particles on a real system perfectly, in many cases the simulation can produce macroscopic results that are accurate enough to be used in applications ranging from determining macromolecular structures to the development of drug delivery systems in the body.[28,29,30]

The potential energy between every pair of particles in the system must be specified to allow the simulation to run. Additionally, a different set of parameters is specified for every type of particle-pair in the system. The functional form of the potentials used for our polymer systems will be discussed in Sections and , and their respective parameters in Section .

Bonded and non-bonded particles are generally also assigned different potentials since such particle pairs behave much differently from each other. As such, we will differentiate between these two potentials, naming them bonded and non-bonded pair potentials respectively.

Bead-Spring Polymer Model

Polymers are commonly modeled using the bead-spring model in MD simulations.[31] This model describes monomers as a single bead instead of a group of atoms, and describes the beads as connected to each other using simple harmonic springs. The advantages of this model is twofold. Firstly, it reduces the complexity of the simulation by reducing the number of particles simulated, thereby allowing us to run larger or longer simulations. This technique of simplifying molecules is known as *coarse-graining* and is very popular amongst computational researchers, and an entire research topic in its own right.[32] The second advantage of this model is that it provides us with a functional form of the potential between bonded particles, i.e.

the bonded potential, which is reasonably accurate in simulating real polymers.[31]

The simple harmonic springs modeling the bonds obey the classical laws of mechanics. As might be expected from physics, the potential energy separating some bonded bead type i and type j as described by a spring is given by

$$V_{ij}(r) = \frac{1}{2}k\left(r - r_0\right)^2 \tag{2}$$

where $V_{ij}(r)$ is the bonded pair potential between i and j, r is their separation, k is the 'spring constant' (representing the stiffness of the spring), and r_0 is the equilibrium length of the spring.[22,23] The two independent variables (which we may change) in this function are k and r_0. These parameters must be chosen for each unique bead pair i, j that are connected with a bond modeled by this potential.

Lennard-Jones Potentials

The 12-6 Lennard-Jones (LJ) potential is one of the most extensively used non-bonding potentials[33] due to its mathematical simplicity allowing for simulation of large systems.[34] It is defined for a pair of particles i and j according to the equation

$$V_{ij} = 4\varepsilon\left[\left(\frac{\sigma}{r}\right)^{12} - \left(\frac{\sigma}{r}\right)^{6}\right] \tag{3}$$

where $V_{ij}(r)$ is the non-bonded pair potential between i and j, r is the separation between the two bodies, ε is the potential well depth, and σ is the finite inter-particle distance where the LJ potential is 0.[35] The potential well depth affects the magnitude of the experienced force at some given separation. ε and σ and parameters chosen for every unique set of i and j in the system.

All bead pairs that were not connected by bonds had their potentials modeled using using LJ potentials.

One interesting point to note is that if these potentials (mainly the LJ non-bonded potential) were to be applied between every pair of non-bonded particles in the system, the number of potentials needed to be calculated would grow on the order of N^2, where N is the number of particles in the system. As such, the complexity of the computation would grow so quickly that even computer simulations would struggle to simulate larger systems containing tens or even hundreds of thousands of particles. To combat this we only calculate potentials between bodies that are within some cutoff radius r_{cut} of each other, which allows the significant interactions to be modeled while considerably reducing complexity of the compuation. The cutoff radius generally set at 2.5σ,[36,37] which captures the most important particle interactions.

Polymer Interaction Parameter

The Flory-Huggins interaction parameter, also known as the polymer interaction parameter or the χ parameter, is a measurement of how favorable the interactions between two different polymer segments is.[1] This interaction parameter is specified as an interaction between two types of polymer segments i and j, and is then denoted χ_{ij}. Generally the interaction parameter is measured from a polymer mixture system either experimentally[38] or from simulations[39] using a myriad of experimental and analytical methods, to produce an expression that is dependent on temperature.[40]

In this study we will define a similar interaction parameter which will be used for quantifying the interaction strength between two different types of monomers in a binary polymer system. In such a system, there are two interactions of importance: self- and cross-monomeric interactions. The greater the self-interactions than the cross-interactions, the more desirable it will be for the polymers to clump up with its own kind. This is intuitively visualized in a system with linear chains, but becomes more interesting when considering systems containing polymers with diblocks or branches.

For our simulations, we will define our own interaction parameter χ which measures the favorability of mixing vs non-mixing (i.e. self vs cross) interactions. Since LJ potentials present the only non-bonded interactions present in our mixture, it is reasonable to define the interaction parameter as a ratio between the strength of LJ interactions, between similar bead types i and i and different-bead types i and j. This is defined as a ratio

$$\chi = \frac{\varepsilon_{ii} \cdot \varepsilon_{jj}}{\varepsilon_{ij}^2}. \tag{4}$$

According to this definition an interaction parameter close to zero implies very unfavorable interactions between like polymer segments which results is favorable segment cross-mixing. A large positive value implies the opposite.

In the original Flory-Huggins interaction parameter however, a negative value ($\chi < 0$) means that the resulting energy of mixing of the segments is favorable, whereas a positive value ($\chi > 0$) means that the mixing is unfavorable.[1] We would like a similar relationship with our defined interaction parameter, which can be emulated by taking the logarithm of the our previous definition to give

$$\chi = \ln\left(\frac{\varepsilon_{ii} \cdot \varepsilon_{jj}}{\varepsilon_{ij}^2}\right), \tag{5}$$

which is negative for favorable mixing ($\varepsilon_{ii}, \varepsilon_{jj} < \varepsilon_{ij}$) and positive for unfavorable mixing ($\varepsilon_{ii}, \varepsilon_{jj} > \varepsilon_{ij}$).

Simulation Parameters

The HOOMD-blue simulation engine is unitless and requires the input parameters to be specified with a set of selfthree fundamental units (distance $\mathcal{D}$, energy $\mathcal{E}$, and mass $\mathcal{M}$), from which all other units are derived.[22,23] For this work the system was modeled with units nm, $\text{kcal}\,\text{mol}^{-1}$, and amu for the three respective fundamental units. Derived units consistent with this set of fundamental units are ps for time, and the Boltzmann constant $k_B = 8.31 \times 10^{-3}\,\text{kJ}\,\text{mol}^{-1}\,\text{Kelvin}^{-1}$. The Boltzmann constant will henceforth be abbreviated as k. Temperature is expressd in terms of the Boltzmann constant as kT.

Both the polymer systems were simulated at a range of temperatures and interaction parameters. The simulations were run in the canonical NVT ensemble, where N refers to the number of particles in the system, V refers to volume, and T refers to temperature, and each of these variables are held constant for the simulation. The simulation is run with the ensemble's corresponding NVT integrator. This ensemble additionally requires a thermostat to keep the temperature constant; the NVT thermostat was used with timestep $\tau = 1.0\,\mathrm{ps}$. This ensemble was chosen due to its ability to stabilize the simulation, allowing for a larger time step to be used.[41] This is useful in studying bead-spring systems such as ours, in which large time periods are required for simulation.

The MD simulation in HOOMD-blue was run with a timestep of 0.001 ps and was allowed to continue for $2 \cdot 10^5$ total timesteps. The last frame of the simulation was analyzed to identify the phase produced at that temperature and interaction parameter, producing a data point for (T, χ). This simulation was repeated for all combinations of temperature $T \in (0.1, 2.5)$ with steps of 0.1 and $\chi \in (-4.0, 4.0)$ in steps of 0.5, providing a total of 425 simulations per polymer system.

The simulation consisted of a rectangular box containing the polymers with periodic boundary conditions. Each bead was initially separated by 1.0 nm in the polymer. Polymers themselves were separated by a center-to-center distance of 2.0 nm. The harmonic bonds holding beads together were all assigned identical equilibrium lengths of 1.0 nm[42] and spring constant $10kT$. As a result, the springs were stiff, allowing the bond length to stay near the equilibrium length.[43,44]

The potential well depths for Lennard-Jones self-interactions (i.e. $\varepsilon_{\mathrm{AA}}$ and $\varepsilon_{\mathrm{BB}}$) were fixed at $2kT$, on the typical order of magnitude for an LJ potential well depth.[45] The the cross-interaction $\varepsilon_{\mathrm{AB}}$ was back-calculated from the this self-interaction and interaction parameter value being investigated as follows:

$$\chi = \ln\left(\frac{\varepsilon_{AA} \cdot \varepsilon_{BB}}{\varepsilon_{AB}^2}\right)$$
$$\implies \varepsilon_{AB} = \sqrt{\frac{\varepsilon_{AA} \cdot \varepsilon_{BB}}{\exp(\chi)}} \tag{6}$$

The σ value was chosen as 1.0 nm. As a result, we set the cutoff radius for these LJ potentials to $2.5\sigma = 2.5\,\mathrm{nm}$.

In order to give a feel for the values of self and cross interactions over the investigated interaction parameter range, values of ε_{AA} and ε_{AB} for some interaction parameters is shown below.

χ	ε_{AA} / kT	ε_{AB} / kT
-3.0	2.0	40.17
-2.0	2.0	14.78
-1.0	2.0	5.44
0.0	2.0	2.00
1.0	2.0	0.73
2.0	2.0	0.27
3.0	2.0	0.10

Results and Analysis

Qualitative Phase Classification

The simulation trajectories were analyzed using the OVITO particle visualization program.[46] As seen in Figures 3 and 4, the types of phases found were related to the homogeneity of monomer distribution inside the simulation box. One phase was defined as a "heterogeneous phase". In this phase distinct "clumps" or "globules" of similar monomers were found. We defined another phase as a homogeneous one, where no such clumps are observed, and there are no more than a few monomers of one type coalescing together. This is characteristic of a situation when cross interactions are more favorable than self interactions. Other phases were classified according to the extent to which they clumped together, which lay somewhere between these two extremes. Various phases in line with the phase descriptions above were investigated in each of the phase descriptions.

Upon investigation of the linear homopolymer blend, certain combinations of temperature and interaction parameter resulted in a heterogeneous phase with like monomers largely separated from each other. This phase was named H1, where H stands for "homogeneous". The other extreme phase contained polymers mixed together homogeneously, named phase H4.

Two more phases in between these extremes, H2 and H3, were observed in the trajectories and named as intermediate phases between H1 and H4. Phase H2 contained relatively large clumps of similar monomers spread throughout the simulation box, while in contrast H1 contained larger clumps that faced a near-binary split. Renders of these phases are shown in Figure 3.

Similar phases can be found in the diblock mixture system, with D1 (with D standing for "diblock") being the most homogeneous and D4 being the most heterogeneous. Intermediate phases called D2 and D3 are also named. These are shown in Figure 4.

Radial Distribution Functions

We consider the radial distribution function, or RDF, denoted as $g(r)$, which describes the density of some particle type B from some other particle type A, averaged across all particles B in the system. Alternatively, it can be thought of as the probability of finding particle A in a volume element at some distance away from a randomly chosen bead B in the system.[47] Hence, the RDF can provide information about the local structure of the system by describing the environment of an average bead of a specific type, with respect to some other bead type.[48] Peaks in the RDF correspond to regions of high density of bead A around bead B.

The RDF can be calculated using

$$\frac{\mathrm{d}n_r}{\mathrm{d}r} = g(r) \cdot 4\pi r^2 \cdot \rho \tag{7}$$

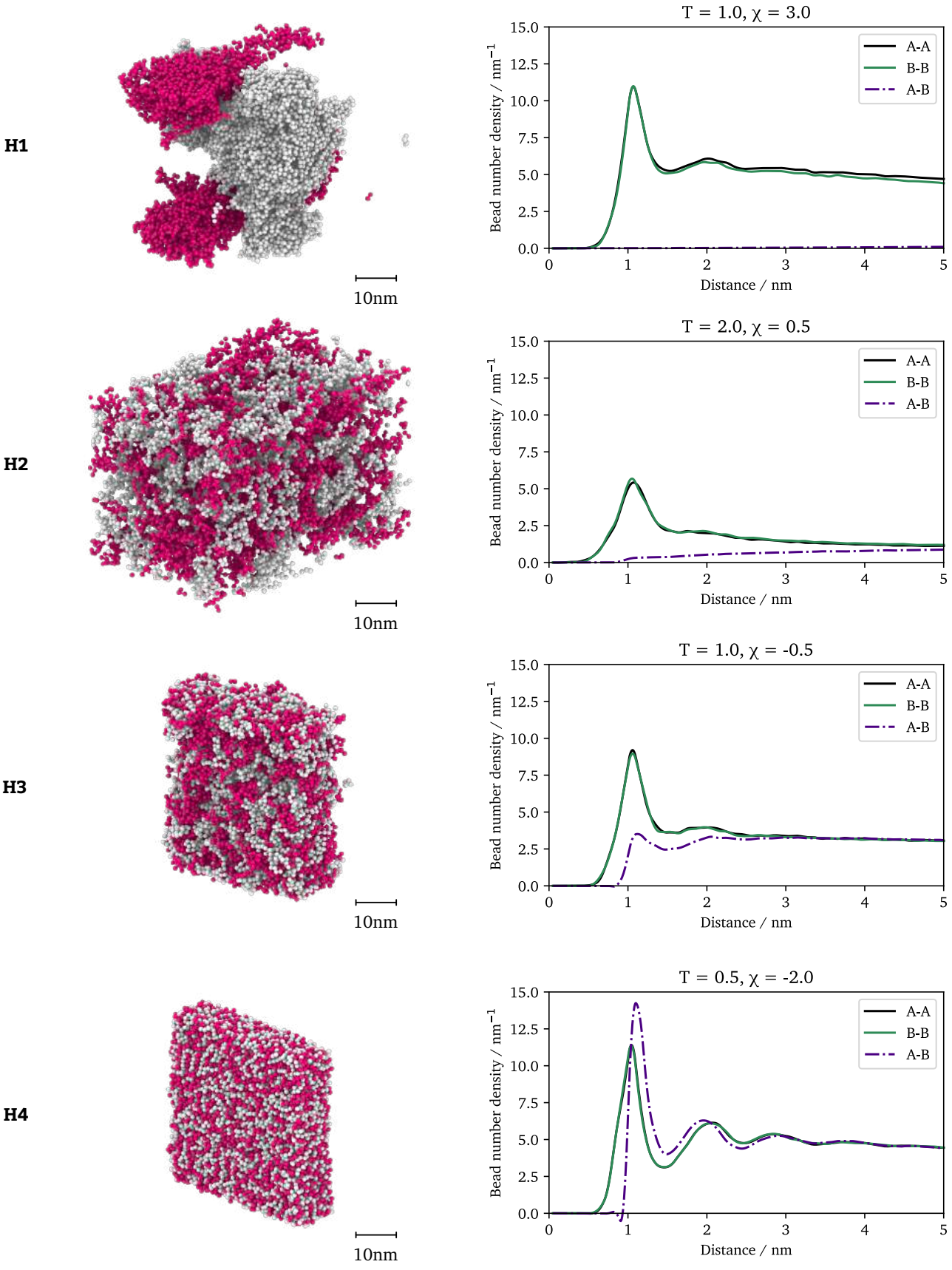

Figure 3. *Simulation renders and RDF diagrams of four simulation trajectories of each of the four identified phases H1-H4. White beads represent bead type A and red ones represent bead type B.*

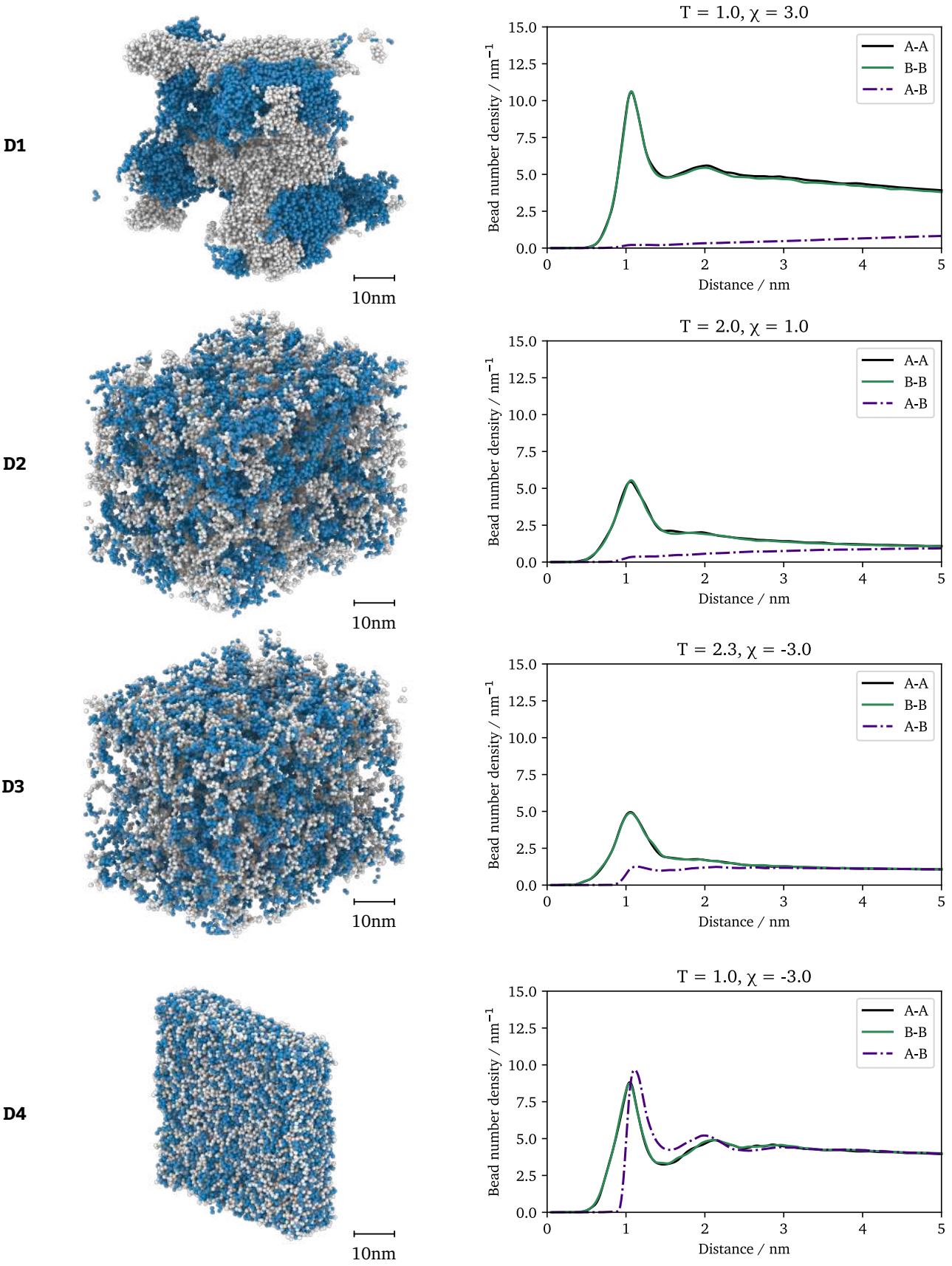

Figure 4. *Simulation render and RDF diagrams phases D1-D4. White beads represent bead type A and blue ones represent bead type B.*

where ρ is the local number density of one bead type around another bead type that the RDF is taken for.[49]

RDF values were calculated for the last frame of each of the phases H1-H4 and D1-D4 using OVITO's coordination analysis modifier.[46] The RDFs are shown in Figures 3 and 4.

For the H1 phase, we observe that the peaks for the A-A and B-B bead-pair RDFs are much higher than that of the A-B bead-pair RDF. This shows that around a distance of about 1 nm away from bead A, there are many other A beads. Likewise, beads of type B preferably congregate around other B beads. The relatively flat curve for the A-B cross-interaction RDF shows that many fewer beads prefer to intermingle with beads of a different type.

For phase H2, we see that, predictably, the peak at for both A-A and B-B RDFs are lower, showing that the like particles tend to be spread out more than in phase H1. This is mainly due to a much higher temperature, giving the system ample energy to spread out, while also lowering the interaction parameter compared to H1 which allows the system to mix better.

In phase H3, we see that the peak increases in size again. This is evident from the snapshot showing the physical characteristic of the polymer blend: it is clumped together in a much smaller volume compared to phase H2. As a result, since beads are closer to each other on average, the density of like particles around other like particles are higher. However, we note that interestingly the A-B RDF start becoming much more significant. This can be explained by the more compact nature of this phase, which prevents polymers of different types from isolating from each other completely, as in phase H1. This is also a result of weaker self and stronger cross interactions.

In the last phase H4, we can see that the cross interactions of beads are more prevalent than self interactions. This is especially interesting as in the original system only beads are bonded to each other.

We can see a similar trend across both systems—that radial distribution functions for corresponding phases have a high level of similarly to each other—suggesting that the systems are similar enough that their own distinct phases do not form.

Although trajectory snapshot renderings are a useful way of visualizing the state and phase of a simulation trajectory, they are not as useful when investigating the phase across a large numbers simulations as we have done in this work across a large range of phase space. For easier visualization of trajectories across a parameter range, we may create a phase diagram that is visual in nature, on which head-on images of the trajectory are overlaid onto the phase diagram. This is performed for both systems to produce Figures 5 and 6.

As we can see, there are definitive transitions between systems that contain polymers clumped together versus those where the polymers are thoroughly mixing. The region around $T = 0.8kT$, $\chi = 2.5$ best shows the phase separation. This is reasonable; at moderate temperatures and strong self-interaction parameters one would not expect the polymers to mix very well. At lower temperatures we see less mixing. This could possibly be due to insufficient time spent running the simulations, as at low temperatures the system would take longer to equilibrate. At much higher temperatures such as $T = 2.0kT$, although clumps of polymers can be seen, the system looks much more chaotic with beads intermingling. This falls in line with what is expected from greatly increasing the internal energy of the system.

The diblock copolymer phase diagram shares much of the characteristics of the homopolymer diagram with some notable differences. Firstly, when overlaying the two phase diagrams, one can see that the region where the phases separate is shifted further to the left. Furthermore, regions appear at lower temperatures which seem to be more separated than the simulations on the linear homopolymer system.However, at high temperatures, this system breaks down and we see mostly homogeneous systems, especially at the negative interaction parameters which favor cross interactions.

Conclusion

In this study, we have observed the effect of changing two variables, temperature and interaction parameter between beads, of two-bead polymer systems. These two systems were seen to behave similarly to each other in terms of phases and the temperature/interaction parameter sets which resulted in them. Four different phases were identified for each system. The RDFs of each phase were inspected to investigate the spacial relationship between like and unlike beads for each phase, and how this realted to the mixing of the two polymers.

A phase diagram was created to investigate the systems further across all of the simulated trajectories. Clear regions were seen that favored polymer separation; at moderate temperatures and positive interaction parameters more significant clumping was seen across both systems. Mixing occurred best at conditions straying further from these moderate conditions, and at negative values of the interaction parameter. The diblock copolymer system seemed to separate more aggressively, but did so at a smaller temperature range. The effect of high temperature and negative interaction parameter on the distribution of beads was also discussed.

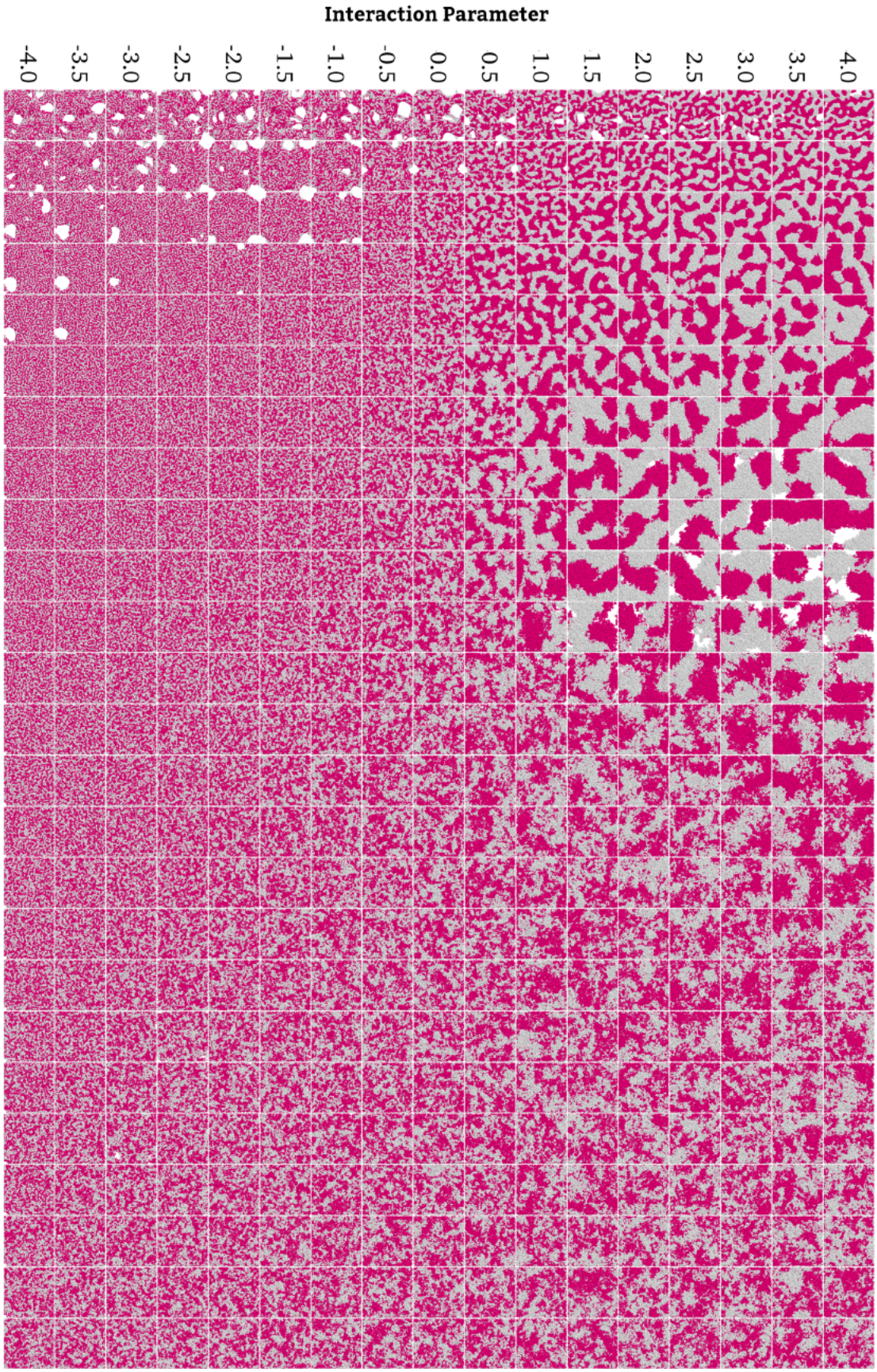

Figure 5. Visual phase diagram for linear homopolymer blend.

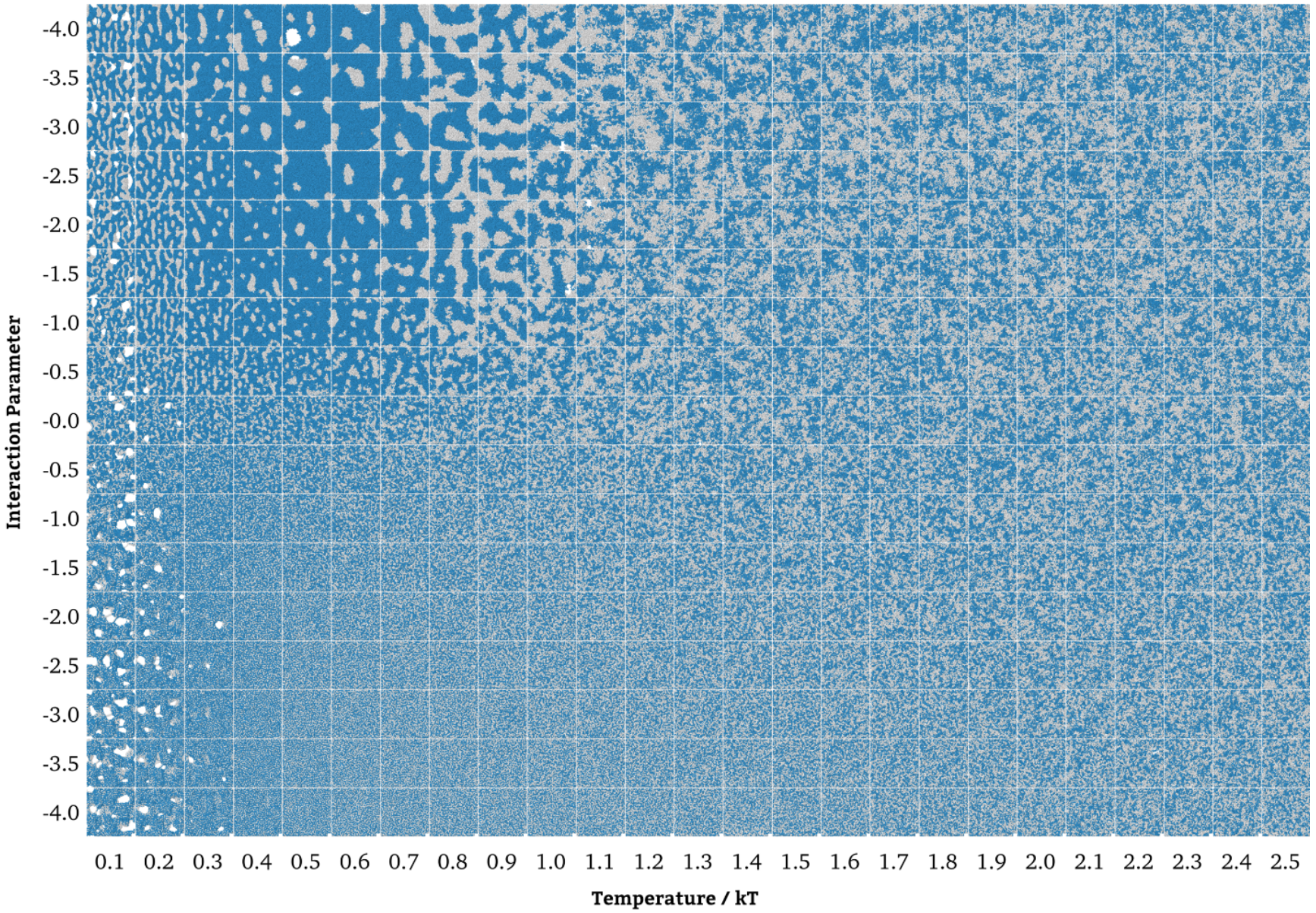

Figure 6. *Visual phase diagram for diblock copolymer blend.*

1 References

[1] F. S. Bates, "Polymer-polymer phase behavior," *Science*, vol. 251, no. 4996, pp. 898–905, 1991.

[2] R. Koningsveld, R. Koningsveld, W. H. Stockmayer, and E. Nies, *Polymer phase diagrams: a textbook*. Oxford University Press on Demand, 2001.

[3] C. M. Durrani, D. A. Prystupa, A. M. Donald, and A. H. Clark, "Phase diagram of mixtures of polymers in aqueous solution using fourier-transform infrared spectroscopy," *Macromolecules*, vol. 26, no. 5, pp. 981–987, 1993.

[4] C. Reiffers-Magnani, J. Cuq, and H. Watzke, "Depletion flocculation and thermodynamic incompatibility in whey protein stabilised o/w emulsions," *Food Hydrocolloids*, vol. 14, no. 6, pp. 521–530, 2000.

[5] A. Halperin, M. Kröger, and F. M. Winnik, "Poly (n-isopropylacrylamide) phase diagrams: fifty years of research," *Angewandte Chemie International Edition*, vol. 54, no. 51, pp. 15342–15367, 2015.

[6] B. Wessling, "Dispersion hypothesis and non-equilibrium thermodynamics: key elements for a materials science of conductive polymers. a key to understanding polymer blends or other multiphase polymer systems," *Synthetic metals*, vol. 45, no. 2, pp. 119–149, 1991.

[7] H. Tanaka and T. Nishi, "New types of phase separation behavior during the crystallization process in polymer blends with phase diagram," *Physical review letters*, vol. 55, no. 10, p. 1102, 1985.

[8] V. Ginzburg and A. Balazs, "Calculating phase diagrams for nanocomposites: the effect of adding end-functionalized chains to polymer/clay mixtures," *Advanced materials*, vol. 12, no. 23, pp. 1805–1809, 2000.

[9] S. Ramakrishnan, M. Fuchs, K. S. Schweizer, and C. F. Zukoski, "Entropy driven phase transitions in colloid–polymer suspensions: Tests of depletion theories," *The Journal of chemical physics*, vol. 116, no. 5, pp. 2201–2212, 2002.

[10] I. Teraoka, *Polymer Solutions: An Introduction to Physical Properties*. Wiley, 2004.

[11] A. Noshay and J. E. McGrath, *Block copolymers: overview and critical survey*. Elsevier, 2013.

[12] H. Dodiuk and S. H. Goodman, *Handbook of thermoset plastics*. William Andrew, 2013.

[13] F. S. Bates and G. H. Fredrickson, "Block copolymer thermodynamics: theory and experiment," *Annual review of physical chemistry*, vol. 41, no. 1, pp. 525–557, 1990.

[14] I. Nwogbaga, *Characterizing the Spatial Morphologies and Temporal Dynamics of Biologically Inspired Multicomponent Systems*. PhD thesis, Princeton University, 2018.

[15] H. Zhang, H. Wang, W. Zhong, and Q. Du, "A novel type of shape memory polymer blend and the shape memory mechanism," *Polymer*, vol. 50, no. 6, pp. 1596–1601, 2009.

[16] R. D. Groot and T. J. Madden, "Dynamic simulation of diblock copolymer microphase separation," *The Journal of chemical physics*, vol. 108, no. 20, pp. 8713–8724, 1998.

[17] J. Huh, V. V. Ginzburg, and A. C. Balazs, "Thermodynamic behavior of particle/diblock copolymer mixtures: Simulation and theory," *Macromolecules*, vol. 33, no. 21, pp. 8085–8096, 2000.

[18] X. He, M. Song, H. Liang, and C. Pan, "Self-assembly of the symmetric diblock copolymer in a confined state: Monte carlo simulation," *The Journal of Chemical Physics*, vol. 114, no. 23, pp. 10510–10513, 2001.

[19] Q. Wang, P. F. Nealey, and J. J. de Pablo, "Monte carlo simulations of asymmetric diblock copolymer thin films confined between two homogeneous surfaces," *Macromolecules*, vol. 34, no. 10, pp. 3458–3470, 2001.

[20] T. Geisinger, M. Müller, and K. Binder, "Symmetric diblock copolymers in thin films. i. phase stability in self-consistent field calculations and monte carlo simulations," *The Journal of chemical physics*, vol. 111, no. 11, pp. 5241–5250, 1999.

[21] A. Ivlev, J. Bartnick, M. Heinen, C.-R. Du, V. Nosenko, and H. Löwen, "Statistical mechanics where newton's third law is broken," *Physical Review X*, vol. 5, no. 1, p. 011035, 2015.

[22] J. Glaser, T. D. Nguyen, J. A. Anderson, P. Lui, F. Spiga, J. A. Millan, D. C. Morse, and S. C. Glotzer, "Strong scaling of general-purpose molecular dynamics simulations on gpus," *Computer Physics Communications*, vol. 192, pp. 97–107, 2015.

[23] J. A. Anderson, C. D. Lorenz, and A. Travesset, "General purpose molecular dynamics simulations fully implemented on graphics processing units," *Journal of computational physics*, vol. 227, no. 10, pp. 5342–5359, 2008.

[24] J. D. Durrant and J. A. McCammon, "Molecular dynamics simulations and drug discovery," *BMC biology*, vol. 9, no. 1, pp. 1–9, 2011.

[25] S. Nosé and M. Klein, "Constant pressure molecular dynamics for molecular systems," *Molecular Physics*, vol. 50, no. 5, pp. 1055–1076, 1983.

[26] M. E. Tuckerman, J. Alejandre, R. López-Rendón, A. L. Jochim, and G. J. Martyna, "A liouville-operator derived measure-preserving integrator for molecular dynamics simulations in the isothermal–isobaric ensemble," *Journal of Physics A: Mathematical and General*, vol. 39, no. 19, p. 5629, 2006.

[27] M. R. Pitman and R. I. Menz, "Methods for protein homology modelling," in *Applied Mycology and Biotechnology*, vol. 6, pp. 37–59, Elsevier, 2006.

[28] J. M. Goodfellow, *Molecular dynamics: applications in molecular biology*. Macmillan International Higher Education, 1991.

[29] W. F. Van Gunsteren and H. J. Berendsen, "Computer simulation of molecular dynamics: methodology, applications, and perspectives in chemistry," *Angewandte Chemie International Edition in English*, vol. 29, no. 9, pp. 992–1023, 1990.

[30] M. N. Al-Qattan, P. K. Deb, and R. K. Tekade, "Molecular dynamics simulation strategies for designing carbon-nanotube-based targeted drug delivery," *Drug Discovery Today*, vol. 23, no. 2, pp. 235–250, 2018.

[31] D. Kozuch, W. Zhang, and S. Milner, "Predicting the flory-huggins χ parameter for polymers with stiffness mismatch from molecular dynamics simulations," *Polymers*, vol. 8, no. 6, p. 241, 2016.

[32] M. G. Saunders and G. A. Voth, "Coarse-graining methods for computational biology," *Annual review of biophysics*, vol. 42, pp. 73–93, 2013.

[33] Z. Li, D. Cao, and J. Wu, "Density-functional theory and monte carlo simulation for the surface structure and correlation functions of freely jointed lennard-jones polymeric fluids," *The Journal of chemical physics*, vol. 122, no. 17, p. 174708, 2005.

[34] H. Heinz, R. Vaia, B. Farmer, and R. Naik, "Accurate simulation of surfaces and interfaces of face-centered cubic metals using 12- 6 and 9- 6 lennard-jones potentials," *The Journal of Physical Chemistry C*, vol. 112, no. 44, pp. 17281–17290, 2008.

[35] L. Verlet, "Computer" experiments" on classical fluids. i. thermodynamical properties of lennard-jones molecules," *Physical review*, vol. 159, no. 1, p. 98, 1967.

[36] C. Batistakis and A. Lyulin, "Simulated glass transition in thin polymer films: Influence of truncating the non-bonded interaction potentials," *Computer Physics Communications*, vol. 185, no. 4, pp. 1223–1229, 2014.

[37] B. Smit, "Phase diagrams of lennard-jones fluids," *The Journal of Chemical Physics*, vol. 96, no. 11, pp. 8639–8640, 1992.

[38] C. Clarke, A. Eisenberg, J. La Scala, M. Rafailovich, J. Sokolov, Z. Li, S. Qu, D. Nguyen, S. Schwarz, Y. Strzhemechny, *et al.*, "Measurements of the flory- huggins interaction parameter for polystyrene- poly (4-vinylpyridine) blends," *Macromolecules*, vol. 30, no. 14, pp. 4184–4188, 1997.

[39] A. Arora, N. Pillai, F. S. Bates, and K. D. Dorfman, "Predicting the phase behavior of abac tetrablock terpolymers: Sensitivity to flory–huggins interaction parameters," *Polymer*, vol. 154, pp. 305–314, 2018.

[40] A. Chremos, A. Nikoubashman, and A. Z. Panagiotopoulos, "Flory-huggins parameter χ, from binary mixtures of lennard-jones particles to block copolymer melts," *The Journal of chemical physics*, vol. 140, no. 5, p. 054909, 2014.

[41] T. Soddemann, B. Dünweg, and K. Kremer, "Dissipative particle dynamics: A useful thermostat for equilibrium and nonequilibrium molecular dynamics simulations," *Physical Review E*, vol. 68, no. 4, p. 046702, 2003.

[42] A. Schlijper, P. Hoogerbrugge, and C. Manke, "Computer simulation of dilute polymer solutions with the dissipative particle dynamics method," *Journal of Rheology*, vol. 39, no. 3, pp. 567–579, 1995.

[43] H. Chen and A. Alexander-Katz, "Polymer-based catch-bonds," *Biophysical journal*, vol. 100, no. 1, pp. 174–182, 2011.

[44] A. Milchev and K. Binder, "Osmotic pressure, atomic pressure and the virial equation of state of polymer solutions: Monte carlo simulations of a bead-spring model," *Macromolecular theory and simulations*, vol. 3, no. 6, pp. 915–929, 1994.

[45] S. H. Lee and P. J. Rossky, "A comparison of the structure and dynamics of liquid water at hydrophobic and hydrophilic surfaces—a molecular dynamics simulation study," *The Journal of chemical physics*, vol. 100, no. 4, pp. 3334–3345, 1994.

[46] A. Stukowski, "Visualization and analysis of atomistic simulation data with ovito–the open visualization tool," *Modelling and Simulation in Materials Science and Engineering*, vol. 18, no. 1, p. 015012, 2009.

[47] B. H. Zimm, "The scattering of light and the radial distribution function of high polymer solutions," *The Journal of Chemical Physics*, vol. 16, no. 12, pp. 1093–1099, 1948.

[48] J. C. Hower, Y. He, M. T. Bernards, and S. Jiang, "Understanding the nonfouling mechanism of surfaces through molecular simulations of sugar-based self-assembled monolayers," *The Journal of chemical physics*, vol. 125, no. 21, p. 214704, 2006.

[49] D. Chandler, *Introduction to modern statistical mechanics*. 1987.

Review: Deep Brain Stimulation as Treatment for Obsessive Compulsive Disorder and Suggested Targets

Michaela Alarie '21, *Biomedical Engineering*

Advised by Sarah McConnell PhD, *Department of Neuroscience*

Background & Significance

Mental disorders have become increasingly diagnosed worldwide. Up to 50% of all Americans will meet clinical criteria for a mental disorder within their lifetime. Despite this unnerving statistic, existing treatments for psychiatric disorders remain limited, and even treatments deemed successful by medical practitioners fail to fully rid patients of their symptoms. This review describes Obsessive Compulsive Disorder, an anxiety disorder, and investigates a relatively new approach to treating patients for whom traditional methods are not effective.

Obsessive Compulsive Disorder (OCD) is an anxiety disorder characterized by obsessions and/or compulsions. Obsessions are defined as intrusive thoughts, images, or impulses, and compulsions are repetitive behaviors such as hand washing or checking clocks. Another clinical characteristic of this disorder is that the obsessions and/or compulsions are significantly distressing and impairing to the afflicted individual. For example, an individual with OCD may believe that they are in some way contaminated and, as a result, feel the impulse to wash their hands constantly. The individual could wash their hands two or even twenty times until their obsession subsides despite significant distress and skin irritation.

There are three main theories of how OCD is manifested. The most noteworthy theory is that abnormalities within the cortico-striatal-thalamic-cortical circuit (CSTC) in the brain are suggested to trigger OCD symptoms. This circuit is responsible for movement selection and inhibition as well as reinforcement and reward. It is hypothesized that OCD is related to hyperactivity of this particular pathway, leading to repetitive behaviors. Secondly, irregularities within the serotonin system or other neurochemical disruptions have been theorized as causes of OCD. Studies have shown that particular selective serotonin reuptake inhibitors (SSRIs) would result in reduced symptoms for OCD patients; however, no specific abnormality in the serotonin system has been identified as a direct cause to date. Lastly, genetics have been noted as a factor contributing to OCD manifestation, as confirmed by twin studies.

Similarly, three treatment methods exist for those with OCD. The most common is pharmacotherapy through use of SSRIs to target serotonin deficiency. However, these drugs have not been consistently effective in treating OCD. Secondly, psychotherapy has proven to be an effective approach in treating OCD symptoms. Specifically, psychotherapy exposes individuals to fearful stimuli with the aim of adaptation of the CSTC pathway to that stimuli. However, the underlying mechanism is not fully understood, and many patients are still resistant to this treatment. In extreme cases, a more invasive approach is ablative procedures, where portions of the CSTC pathway are lesioned to reduce symptoms.

While current treatments have shown moderate success, 10-20% of people with OCD still experience negative symptoms after treatment. Deep brain stimulation (DBS) has been recently adopted as an additional treatment option, after its success in treating movement disorders such as Parkinson's Disease. DBS is an invasive neurosurgical approach involving implantation of electrode arrays into specific regions of the brain. These regions are reached via drilled holes (also known as burr holes) in the skull, where the array is guided via neuroimaging. The electrodes then provide electrical stimulation to the desired target to correct abnormal activity in circuitry such as the CSTC pathway. DBS treatments vary by the specific target in which electrodes are placed. In this paper, two DBS targets will be discussed: the nucleus accumbens (NA) and the ventral anterior limb of the internal capsule and ventral striatum (VC/VS).

Nucleus Accumbens

One such study targeted the NA of two subjects suffering from chronic, treatment-resistant OCD. This target was chosen as the nucleus accumbens responds to unpredictable stimuli by halting any ongoing behaviors. Therefore, a hyperactive NA would result in a fixed pattern of thoughts and actions which are typical OCD symptoms.

Inclusion criteria for this study involved severe and treatment-resistant OCD with a duration of at least five years, involving failed attempts of psychotherapy, pharmacotherapy, ECT, and augmentation strategies (i.e. antipsychotics). Yale-Brown Obsessive Compulsive Scale (Y-BOCS), a scale to assess OCD severity, and General Assessment of Functioning Score (GAF), a scale that measures mental health, were conducted preoperatively. To be included in the study, patients must have presented a preoperative Y-BOCS score greater than 30 (out of 40) and GAF of less than 45 (out of 100).

Electrodes provided electrical stimulation to the NA. These were implanted surgically via a cannula inserted through cranial burr holes in each hemisphere, 10mm above the NA. Postoperative CT scanning was then used and compared to preoperative MRI scanning to confirm accurate targeting

with the electrodes. While reasoning for different pre- and post-operative imaging modalities was not indicated, it is inferred that an MRI was not used postoperatively, as metallic electrodes would result in serious complications for the patient through magnetic attraction out of the brain. Finally, stimulation was provided, given that voltage amplitudes above 5V delivered therapeutic effects.

Postoperatively, Patient 1 demonstrated a decreased Y-BOCS score (38 to 22), with an increase in GAF score (40 to 60). Similarly, Patient 2 demonstrated a decreased Y-BOCS score (30 to 20) with an increase in GAF score (40 to 60). Overall, both patients experienced significant psychological improvement of OCD symptoms.

Strengths and Weaknesses

DBS targeting the NA has many advantages over other treatments. Firstly, this procedure is reversible, as compared to ablative treatment. Although implantation involves production of burr holes, the electrodes can be removed from the brain with minimal tissue damage. If the treatment is considered ineffective, it can be "reversed" unlike ablative surgeries which permanently remove or lesion pieces of the brain. This presents a more attractive strategy for both medical professionals and patients. Secondly, this approach provides electrical stimulation to correct any disruptions to neural circuitry in real time. This potentially suggests a cure for patients rather than a treatment that only decreases the severity of the disorder. However, there are some potential issues with using constant stimulation to treat a psychiatric disorder. In this method, researchers assume that each psychiatric episode experienced by the afflicted individual is the same. If a patient is experiencing a major episode, this may require more stimulation than required for a particularly mild episode.

In spite of promising results, the study did not report long term efficacy of the treatment. This is particularly concerning since the authors stated that Patient 2 had minimal results for the first two years of testing (in which the patient was tested for only three months longer than that time period). Patient 2 was not demonstrating significant clinical recovery due to a dead battery as well as an imprecise location targeted within the nucleus accumbens. While the patient experienced an impressive and quick increase in functioning after correcting this, the device was only effective between the 24- and 27-month period, and the data may be insufficient to draw a particular conclusion regarding device efficacy. The subjects were not given an opportunity to qualitatively assess the ability of DBS to reduce their own symptoms. While clinical measures like Y-BOCS and GAF showed a change in score after the procedure, verbal reports of overall functioning could have supplemented the data demonstrating clinical improvement. These verbal reports could have provided further insight into the occurrence of intrusive thoughts in addition to feelings of device efficacy (such as if patients are uncomfortable or experiencing any adverse symptoms with regard to the device itself).

Ventral Anterior Limb of the Internal Capsule and Ventral Striatum

Targeting the ventral anterior limb of the internal capsule and ventral striatum for electrical stimulation serves as an alternative DBS target for OCD symptoms. In a study conducted by Greenberg et al. (2010), this target was chosen due to its function as a node in the cortico-striatal-thalamic-cortical (CSTC) pathway. Previously mentioned, hyperactivity within the CSTC is one of the primary causes of OCD symptoms. Therefore, correction of this abnormality via one of the nodes in this pathway is a logical target for DBS.

This study presents data collected from patients over the past eight years from four different groups: Leuven/Antwerp, Butler Hospital, Cleveland Clinic and University of Florida. Overall, 26 patients were studied. With regard to patient characteristics, ages ranged from 7 to 34 years old, and 20 of the 26 patients developed OCD by the age of 18. Additionally, psychological measures were predetermined via Y-BOCS (mean score 34.0 out of 40.0), Hamilton Anxiety Rating Scale (HAM-A; mean score 22.1 out of 56.0) and GAF (mean score 34.8 out of 100.0, excluding the University of Florida Group scores). Exclusion criteria involved a history of a psychotic disorder, a manic episode in the past three years, and a significant neurological disorder or abnormality. Additionally, patients must have demonstrated clear treatment-resistance. This involved a minimum of twenty sessions of behavioral therapy as well as at least three months of pharmacotherapy (SSRIs).

The device used in the study consisted of leads containing four cylindrical electrode contacts, each 3mm long, spaced 4mm apart, and could be set as positive, negative, or off. As more subjects were tested in this study, the leads were placed more posteriorly based on the clinical benefit observed for this approach. Postoperative imaging (CT) was then utilized to determine correct placement of the leads. Testing was performed postoperatively to discern the effectiveness of the electrodes, in which stimulation was provided separately to each electrode, ranging from 2 to 8V. Patients were also instructed to provide verbal feedback of any adverse effects as well as alterations in mood, thinking, or motor function.

For data analysis, the subjects were categorized into three groups: early (Group A; January 2002), midterm (Group B; April 2003), and most-recent (Group C; March 2005) implantation, each with a slightly different implantation site. Post-DBS, the previous psychological measures (Y-BOCS, HAM-A, GAF) were re-recorded at 1-, 3-, 6-, 12-, 24-, and 36-month intervals. Across all groups, it was observed that Y-BOCS score decreased from the original 34.0 to 21.0, demonstrating symptom relief. Of the three groups, Groups B and C, which had more posterior sites, obtained the greatest Y-BOCS decrease (53.9% and 54.3% decreases respectively). This indicates that a more posterior approach is in fact indicative of a greater therapeutic effect. Secondly, the mean GAF increased from baseline value of 34.8 to 53.9 at 36

months. Finally, similar to Y-BOCS, it was observed that the HAM-A score for the groups as a whole decreased from the baseline by an average of 58.7% by 36 months.

Strengths and Weaknesses

A major strength in stimulating posterior regions of the VC/VS is that it directly stimulates a node within the CSTC, which is a siteattributed to symptoms of OCD. Additionally, electrical stimulation presents a less drastic, although arguably equally invasive, approach than cingulotomy. Implantation of electrodes can reduce symptoms by correcting existing brain circuits, rather than lesioning and destroying them. However, a drawback to this approach is that implantation of electrodes raises the possibility of procedure-related complications. In fact, these did occur in the study, where two patients experienced intracerebral hemorrhage, one experienced a tonic-clonic seizure and another experienced a superficial wound infection.

This study gives a compelling case for DBS in the VC/VS, not only looking at a larger sample than previously discussed, but also considering their clinical narratives. These narratives involved verbal feedback for three functional categories: work, school, or homemaking; independent living and activities of daily living; and social engagement. While the anxiety scales provide important quantitative data, it was valuable to observe qualitative data to recognize how patients personally feel about their progress, which is often not included in psychiatric studies. Unfortunately, patient improvements cannot be clearly attributed to DBS because of the allowance of concurrent treatments. In addition to DBS, some patients also were receiving treatment for their OCD via pharmacotherapy and behavioral therapy. While it may be unethical to disrupt all therapies involved in OCD treatment other than DBS, it does pose a potential confounding variable. Although symptoms improved during the time of the study, this could be attributed to sudden effectiveness of one of the other treatments present at the same time.

Comparing Targets

Both studies present consistent results that suggest DBS can aid in alleviating symptoms caused by OCDr; however, the work done with Greenberg et al. (2010) appears to present a stronger approach than Franzini et al. (2010).

While the two studies presented equally suitable targets for DBS, the experimental design and findings from Greenberg et al. (2010) were stronger. Firstly, Greenberg et al. (2010) had a larger population of subjects that were studied over a longer course of time. In their paper, 26 subjects were tested across four labs. Over the eight-year span of the study, each subject was studied for up to 36 months, presenting improved OCD symptoms even within the first three months. Conversely, Franzini et al. (2010) performed DBS on two subjects for approximately two years. Despite this extended length of time, effects were not observed for Subject 1 until a year had passed while Subject 2 presented no results until 22 months, improving then due to better targeting of the NA core after a battery change.

In Greenberg et al. (2010), there were a few complications with regard to side effects of the surgical implantation. As previously stated, two of the 26 patients had small intracerebral hemorrhages: one developed a superficial wound infection, and another experienced a tonic-clonic seizure, indicating some risk involved with the implantation procedure. Nonetheless, a major strength of Greenberg et al. (2010) was the use of verbal feedback from subjects to assess efficacity of the treatment. While measures such as GAF and YBOCS demonstrate clear quantitative information, it is important to also receive qualitative feedback from those tested. This way, it can be even further understood if this treatment is beneficial in improving everyday functionality such as independent living or social engagement.

Future Directions of DBS

Large strides have been made in the past decade to reduce symptoms for those suffering with chronic and severe OCD. However, further studies can be conducted to contribute to this field. Below are examples of future directions presented both from the research articles as well as from the viewpoint of this report.

As mentioned previously, one of the complications from Franzini et al. (2010) was the need to replace the battery of the DBS device. Since replacement must occur every 2-3 years, this presents a limitation to the treatment. Future directions posited by Franzini et al. (2010) involve creating a rechargeable device for which charging would be less invasive than a complete battery replacement. Secondly, an interesting point raised by Greenberg et al. (2010) is the potential influence of varied OCD symptoms on results. While OCD has general symptoms and hallmark characteristics, the specific obsessions and behaviors that individuals experience may differ greatly. To correct this, future studies may conduct a sham-controlled study to observe the possible variability on the effectiveness of DBS as a treatment.

While DBS studies to date have been promising, they have all been "open-loop", meaning that stimulation parameters, such as voltage and frequency, always remain constant. A logical next step would be to provide "closed-loop" electrical stimulation by alteration of stimulation parameters. This can be accomplished through feedback from sensors for neural signatures (biomarkers) that are indicative of particular OCD symptoms. This also proposes the potential to conserve battery life since there will no longer be a constant high voltage.

In order to clarify the efficacy of DBS for OCD, more subjects should be engaged in longitudinal studies. While Greenberg et al. (2010) presented a large number of subjects, there were many changes with regard to electrode placement, which became more posterior over time. Targeting a consistent location across more subjects will increase the confidence in results regarding DBS efficacy. On the other hand, while

there are several studies analyzing the efficacy of DBS in OCD, location of stimulation has varied across studies. These targets have included: VC/VS, NA, subthalamic nucleus, and inferior thalamic peduncle. One future direction could be a study that involves participants receiving DBS of a different target. This way, it can be determined if there is a true "ideal" target of DBS in order to improve the symptoms of those suffering with OCD.

References

Franzini, Angelo, Giuseppe Messina, Orsola Gambini, Riccardo Muffatti, Silvio Scarone, Roberto Cordella, and Giovanni Broggi. "Deep-brain Stimulation of the Nucleus Accumbens in Obsessive Compulsive Disorder: Clinical, Surgical and Electrophysiological Considerations in Two Consecutive Patients." Neurological Sciences 31, no. 3 (2010): 353-59. doi:10.1007/s10072-009-0214-8.

Greenberg, B. D., L. A. Gabriels, D. A. Malone, A. R. Rezai, G. M. Friehs, M. S. Okun, N. A. Shapira, K. D. Foote, P. R. Cosyns, C. S. Kubu, P. F. Malloy, S. P. Salloway, J. E. Giftakis, M. T. Rise, A. G. Machado, K. B. Baker, P. H. Stypulkowski, W. K. Goodman, S. A. Rasmussen, and B. J. Nuttin. "Deep Brain Stimulation of the Ventral Internal Capsule/ventral Striatum for Obsessive-compulsive Disorder: Worldwide Experience." Molecular Psychiatry 15, no. 1 (January 15, 2010): 64-79. doi:10.1038/mp.2008.55.

Holtzheimer, Paul E., and Helen S. Mayberg. "Deep Brain Stimulation for Psychiatric Disorders." Annual Review of Neuroscience 34, no. 1 (2011): 289-307. doi:10.1146/annurev-neuro-061010-113638.

Provenza, Nicole R., Evan R. Matteson, Anusha B. Allawala, Adriel Barrios-Anderson, Sameer A. Sheth, Ashwin Viswanathan, Elizabeth Mcingvale, Eric A. Storch, Michael J. Frank, Nicole C. R. Mclaughlin, Jeffrey F. Cohn, Wayne K. Goodman, and David A. Borton. "The Case for Adaptive Neuromodulation to Treat Severe Intractable Mental Disorders." Frontiers in Neuroscience 13 (2019). doi:10.3389/fnins.2019.00152.

Stein, Dan J. "Obsessive-compulsive Disorder." The Lancet 360, no. 9330 (2002): 397-405. doi:10.1016/s0140-6736(02)09620-4.

This page left intentionally blank.

The Representation of Vowel formants in the Inferior Colliculus due to Singing, Reciting, & Speech

Akshay Sharathchandra '21, Mohammed Abumuaileq '21 & Victoria Figarola '21, *Biomedical Engineering*

Advised by Laurel Carney, *Department of Biomedical Engineering & Neuroscience* and Joyce McDonough, *Department of Linguistics*

Abstract

Hearing is a complex process that activates several regions of the brain. Sound stimuli, including speech and music, are converted from mechanical stimuli to electrical signals through the auditory nerve pathway. This pathway stimulates the cochlear nucleus and inferior colliculus where encoding and processing occur. Speaking, singing, and chanting are identified as popular modes of communication, each of which can be characterized by different rhythms and modulations of vowels. In this investigation, the vowel formant coding of short stimuli, that includes speaking, singing, and reciting was studied across different hearing conditions: healthy, impaired, and impaired with hearing aid. The results have shown that the formants are more clearly visible in the healthy ear and are missing from the impaired ear, especially at higher frequencies. The lack of response at higher frequencies was restored by using a hearing aid.

Background

This investigation was completed as a term project for *BME/LIN 216: Speech on the Brain* in the Spring of 2020. Throughout the class, speech was examined in all of its stages: as words and vowels formed in the mouth, projected across space via invisible waves, taken in by the ear to induce physiological changes, and processed in the ever-complex brain through electrical signals. While brainstorming our project topic, we combined our classroom learning with our passion for music. We were curious about the differences in how humans hear and process different mediums of voice, and how we could use computational modeling to visualize these differences. Due to the coronavirus pandemic, equipment was limited and communication was remote. However, the investigation persisted.

Introduction

Auditory perception is a multi-step process that activates several regions of the brain. A sound stimulus, composed of a wave with a frequency between 20 Hz and 20,000 kHz, is capable of being processed by the human brain in the form of a series of electrical pulses, or action potentials.[1] A sound stimulus first travels through the external and middle ear where it may be filtered and localized before reaching the cochlea, a spiral shaped bone structure, that is tonotopically arranged.[1] Depending on the frequency of the stimulus wave, pressure waves in corresponding regions of the cochlear fluid will cause motion within the basilar membrane of the cochlea, leading to the displacement of inner hair cells (IHCs) and opening of ion channels.[1,2,3]As K^+ and Ca^{2+} ions rush into IHCs, neurotransmitters are released from hair cells to the frequency-specific auditory nerve fibers, thus converting the physical signal of the sound wave into a series of electrical pulses. After leaving the cochlea, these pulses travel along the auditory nerve (AN) from the cochlea to the cochlear nucleus, and later to the inferior colliculus (IC).[1,2] The neurons in the IC are tonotopically arranged in layers, which are the convergence points for several AN fibers.[1] The IC is capable of processing complex sounds such as speech and passes signals along to the thalamus and cortex for further processing.[1,2,4]

The range characteristic of speech is within the aforementioned range of stimulus frequencies detectable by humans. The relative fundamental frequency (F_0) for speech, or the frequency of vibration of vocal cords in the production of speech, is correlated with the size of an individual's body and vocal cords, along with numerous other factors.[5] Therefore, speech from women *generally* has higher F_0 values and has a higher pitch than speech from men.[5]

An important characteristic of speech across several languages is the rhythm of syllable production, which commonly falls between 3-8 syllables per second.[6] This rate is not only limited by the movement of structures involved in the production of noise, such as our tongue, lips, and jaw, but also by the rate at which speech intelligibility saturates within the brain.[6] In addition to speech processing, the IC is also involved in recognizing music, particularly in identifying harmonies.[7] Like speech, singing makes use of vibrations within the vocal cords and carries information through rhythmically defined modulations.[8] Previous studies have noted differences in the ability to perceive speech in patients with amusia, suggesting that there may be an overlap between the encoding involved in speech and music processing. However, these studies have stopped short of examining the specific response patterns with the AN and IC.[6,8]

In this study, the coding of vowel sounds across three different modes of stimuli is examined in the IC under two hearing conditions. Phrases are spoken, sung, and chanted in order to observe the effect of coding from rhythm and pitch modulation on the IC response in a healthy and an impaired ear model. The IC was chosen as an area of focus due to its acute

sensitivity to fluctuations in the AN response which allows for an in-depth view of the differences between the aforementioned methods of communication. When the AN fiber is tuned at a frequency near a vowel's formant, its response envelope becomes flat with almost no fluctuations. This leads to a decreased response, or a dip, in the IC, which indicates the formant. On the other hand, if the AN fiber is tuned to a characteristic frequency (CF) further from the vowels formant, the AN response will be more fluctuated, leading to a higher IC response. It was hypothesized that the vowel formants are more well-encoded in a healthy auditory system. Furthermore, the impaired auditory system with a hearing aid would restore features lost in the impaired ear model, such as the IC response at high CFs and formant representation.

Approach

The approach required several different steps in order to prepare for the analysis, beginning with the formation of different stimuli. Ten different stimuli were presented, constituting three categories: speech, singing, and reciting. The songs chosen to be sung and spoken were the easily recognizable, 'Happy Birthday,' 'Mary had a Little Lamb,' and 'Twinkle Twinkle Little Star.' These recordings were performed by a female speaker. The speech chosen for reciting were short verses from the Qur'an, read by a male speaker as normal speech. Each stimulus was recorded to analyze the speech under three conditions: normal hearing, impaired hearing, and impaired hearing corrected by a hearing aid. To model an individual with a hearing aid, the application 'Ear Machine' was used, with its settings adjusted to a loudness level of 53 and a fine-tuning of -22.[9,10] The sound level was set to 65 dB SPL (sound pressure level) for normal hearing and impaired hearing. However, the sound level for the hearing aid was set to 79 dB SPL. The reader may refer to the recordings in the Appendix to see how this sound level was calculated. The stimuli had different durations depending on the condition being tested.

Each stimulus was recorded using two applications. Using the computer's microphone with no additional settings, the software PRAAT was used for normal and impaired hearing. For the hearing aid recording, the application Ear Machine was used on a phone with fine-tuning and loudness adjusted to -22 and 53.[10] To find the appropriate sound level for the hearing aid condition, two recordings were done on Ear Machine with the values of loudness and fine-tuning (53, -22) chosen to mimic a hearing aid setting. The second recording used the setting for normal hearing, with a loudness of 18 and fine-tuning of 0. The difference between the two sound levels of the recordings was computed and added to 65 dB SPL (normal hearing sound level). Therefore, the sound level for the Ear Machine was found to be 79 dB SPL.

Each stimulus was then input into two computational models: Zilany et al. (2014) and Nelson & Carney (2004). The Zilany et al. (2014) framework models the auditory nerve (AN) and is able to assess practical neural encodings with a variety of characteristic frequencies.[10] The Nelson & Carney (2004) framework models the inferior colliculus (IC), which measures the change in temporal envelopes.[11] The IC neurons have modulation filters that are tuned at a specific frequency, best modulation frequency, which is usually around 100 Hz. These filters are similar in shape to a bell curve that is centered at 100 Hz. The IC cells studied in this experiment are band enhanced (BE). In general, the maximum response is obtained at the modulation frequency. When the pitch of the person varies away from 100 Hz, the response of the IC decreases accordingly. Furthermore, the IC cells are very sensitive to fluctuations in the AN response. The AN response has a flat envelope when the characteristic frequency of the AN fiber is near a formant, leading to a low IC response. When the characteristic frequency of the AN fiber is not near a formant, the AN response fluctuates, resulting in a stronger IC response.

Once the stimuli were entered into the auditory models (IC and AN), the number of characteristic frequencies was changed to 40 to obtain smoother responses with a range of 200 to 3000 Hz. To analyze normal hearing, the audiogram values remained 0 dB HL (hearing level). However, to analyze impaired hearing in an individual, the audiogram values were changed to 35, 35, 38, 40, 40, 60, and 75 dB HL.The audiogram values used for impaired hearing were also used for the hearing aid. The IC and AN responses were observed under a wide display, which is a property of the models used that illustrate the AN and IC responses for sentences, and the rates (spikes/second) were observed for both the AN fiber and IC BE Model. Using the wide display, the dips in the AN and IC were seen more clearly. The dips in the IC occurred at the formants of the vowel of each word.

One of the main advantages of this technique was the ability to look at specific parameters and choose to examine one particular part of the brain. However, there was a small sample size, as only two subjects were recorded, one of each gender. To produce more accurate results, a larger sample pool of individuals could be recorded, as individuals speak and say vowels differently due to gender and accents.

Results

Reciting and Speaking: Reciting

In this section, two verses from the Qur'an were spoken and recited in order to study the effect of vowel representation in the IC response. The verses were, "Qul a'udhu birabbin naas, Malikin naas," which roughly translates to, "Say: I seek refuge with the Lord of mankind, the King of mankind." The following results represent the AN and IC responses to spoken and recited verses in healthy, impaired, and impaired with hearing aid models.

The responses of a healthy auditory system to spoken and recited Quranic verses have been plotted in Figures 1 and 2. Different features shown in the IC response indicate several attributes, such as the vowel formants represented by the red circles, fricatives shown by the black circles, and phase-locking to the fundamental frequency indicated by the white arrows. The red circles, or the vowel formants, are more evident in

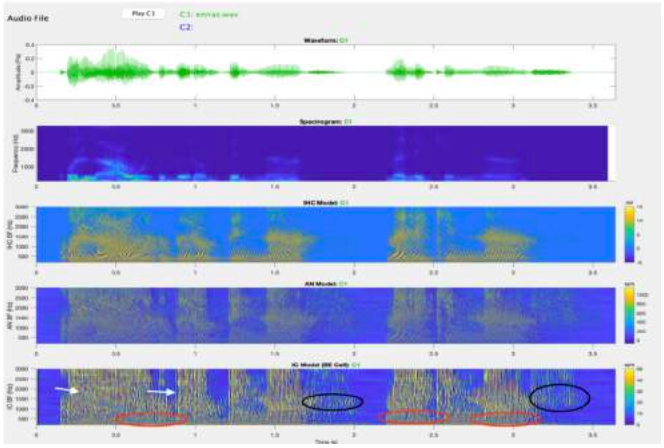

Fig. 1) AN and IC model outputs to two spoken sentences from the Quran. The last two plots represent the AN and IC responses, respectively. The vertical yellow stripes indicate that the IC responses are phase-locked to the fundamental frequency, or the pitch, of the speaker.

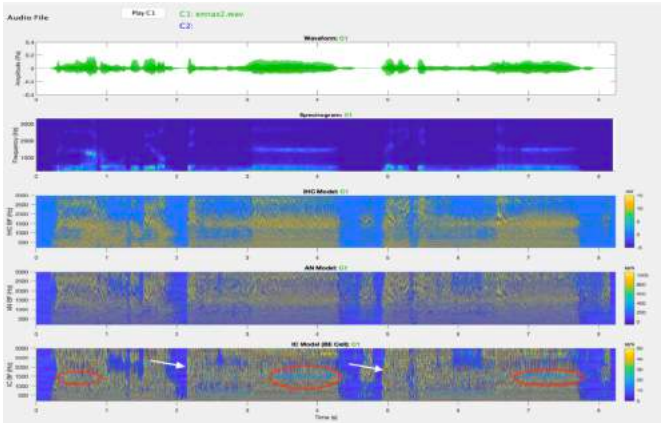

Fig. 2) The outputs of a healthy ear AN and IC model to two recited sentences from the Quran.

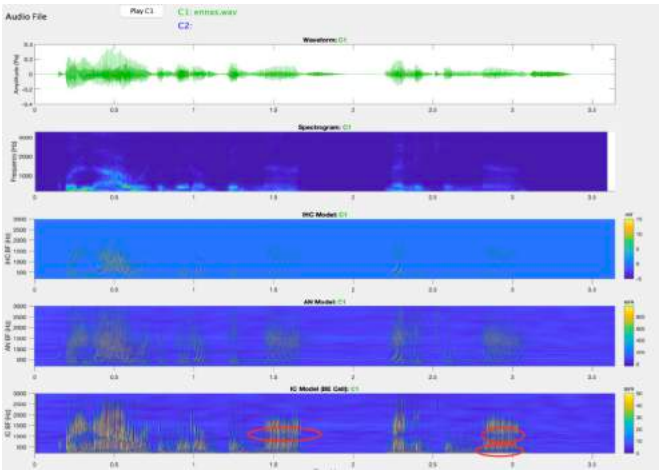

Fig. 3) The outputs of the impaired ear AN and IC models for two spoken sentences from the Quran.

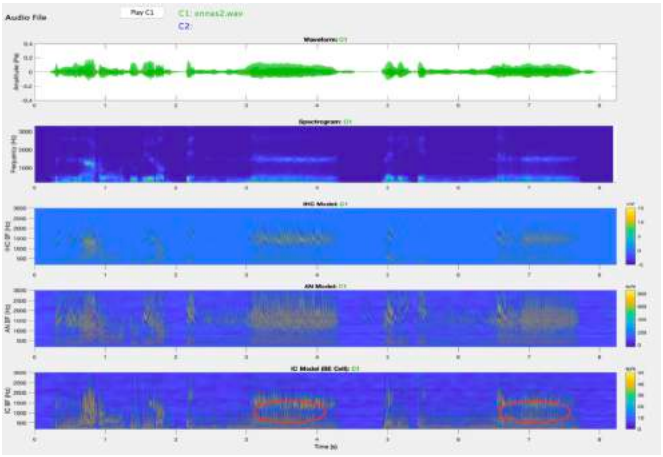

Fig. 4) The outputs of the impaired ear AN and IC models for two recited sentences from the Quran.

Figure 2 than in Figure 1 because the vowels were prolonged when recited.

The responses of an impaired auditory system to spoken and recited Quranic verses are plotted below in Figures 3 and 4. A lack of response at high frequencies has been noted; this is because the audiogram had been set to high hearing thresholds at higher frequencies. As shown in Figure 3, hearing loss causes a severe decrease in the IC response. However, some vowels' formants are still seen as indicated by the red circles. In Figure 4, the formants were still apparent; however, there were fewer bright responses due to less phase-locking to the fundamental frequency as the pitch increases in reciting.The responses of an impaired auditory system with Ear Machine to spoken and recited Quranic verses are plotted below in Figures 5 and 6. The lack of response to high CFs, as previously noted in Figures 3 and 4, has not been observed in Figures 5 and 6 below due to the fact that Ear Machine emphasizes the high frequency components of the sound. In Figure 5, the formants are still shown at very low frequencies.

Reciting and Speaking: Speaking

The sentences used to analyze the responses on the vowels were: (a) 'Happy Birthday to You', (b) 'Twinkle Twinkle Little Star', and (c) 'Mary had a Little Lamb.' In Figures 7 and 8, the results for speaking and singing depict the first second in 'Mary had a Little Lamb', which focuses on the word 'Mary.'

Figure 7 below represents the spectrogram using PRAAT to find the values for the average and single point for the intensity, pitch, and three formants, which can be seen in Table I. Figure 7 represents the word and vowel in 'Mary', as in 'Mary had a Little Lamb.' In Figure 7a, the blue line represents the average pitch, the yellow line represents the average intensity, and the red dots signify the formants across the entire word.

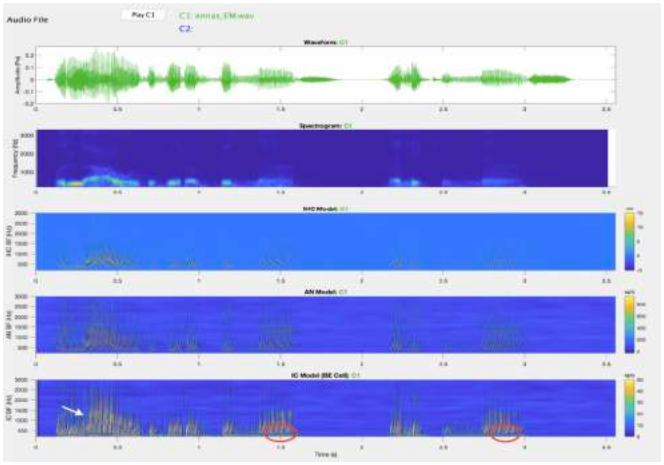

Fig. 5) The with AN and IC model responses for an impaired ear with hearing aid to two spoken sentences. Phase-locking is pointed out by the white arrow.

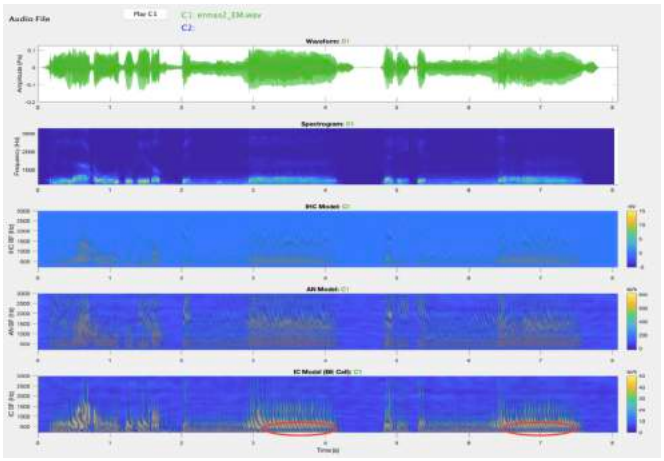

Fig. 6) The with AN and IC model responses for an impaired ear with hearing aid to two recited sentences.

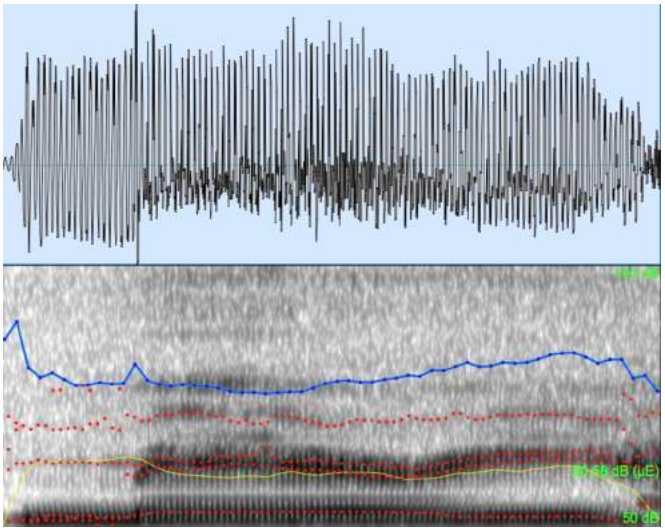

Fig. 7a) The average intensity, pitch, and formants across the word 'Mary'

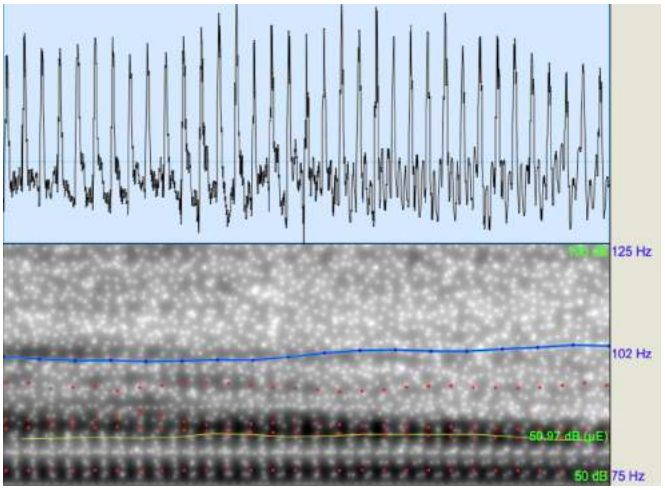

Fig. 7b) The specific intensity, pitch, and formants for the vowel 'a' in 'Mary'

Figure 7b represents the vowel 'a' in 'Mary,' showing the exact intensity, pitch, and formants.

In Figure 7b, the pitch and intensity lines are more linear than in 7a, as only the vowel is being analyzed. Additionally, the formants are more aligned to the 'a' in 'Mary,' rather than the entire word.

Table I separates the word containing the vowel, the intensity (dB), the pitch (F_0), and three formants of the words containing vowels in the sentences above. The values were measured on PRATT using the spectrogram and compared to the dips seen in the IC model. The dips on the IC model depict the fluctuations when the vowel is heard. On PRATT, the measurements were found automatically by using the functions of pitch, intensity, and formant listings at the vowel, which are bolded and italicized in the table below. Additionally, the intensity, pitch, and formants are measured at a single point: the vowel itself.

For the three songs spoken, strong dips can be seen on the vowel of the words for the healthy hearing condition. Figure 8 below depicts the speaking responses in the IC for the vowel 'a' in 'Mary' (the first second) for normal hearing, impaired hearing, and hearing aid (Ear Machine). Both the impaired hearing and the hearing aid have a much weaker IC response. Dips are still noticeable for the first formant, but not the rest. Impaired hearing has a weaker response than the hearing aid. This is due to the fact that the hearing aid amplifies the sound and thus has a higher sound level (79 dB SPL).

Singing

The table above separates the word containing the vowel, the intensity (dB), the pitch (F_0), and the three formants of the

Table I: Intensity (dB), pitch (F_0), and the formants (Hz) of the spoken words containing vowels for normal hearing.

Word	Intensity (dB)	Pitch (F0) (Hz)	F1 (Hz)	F2 (Hz)	F3 (Hz)
H***a***ppy	57.88	102.00	920.0	1812	2812
B***i***rthday	54.09	96.59	506.0	1726	2341
M***a***ry	59.97	102.00	596.0	2068	2760
L***i***ttle	57.09	93.74	472.0	1685	3026
L***a***mb	56.52	90.26	762.0	2062	2627
Tw***i***nkle	62.79	109.10	451.0	2485	3167
L***i***ttle	55.66	97.10	531.8	1921	2958
St***a***r	54.98	95.53	578.0	1352	2559

Fig. 8) IC Responses to speaking 'Mary had a Little Lamb':

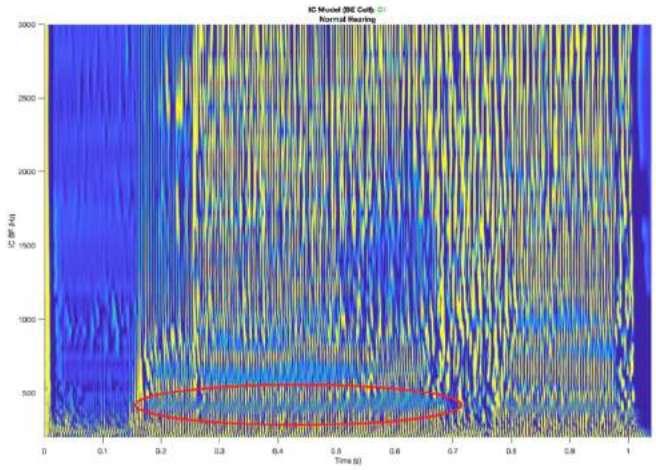

Fig. 8a) Normal Hearing

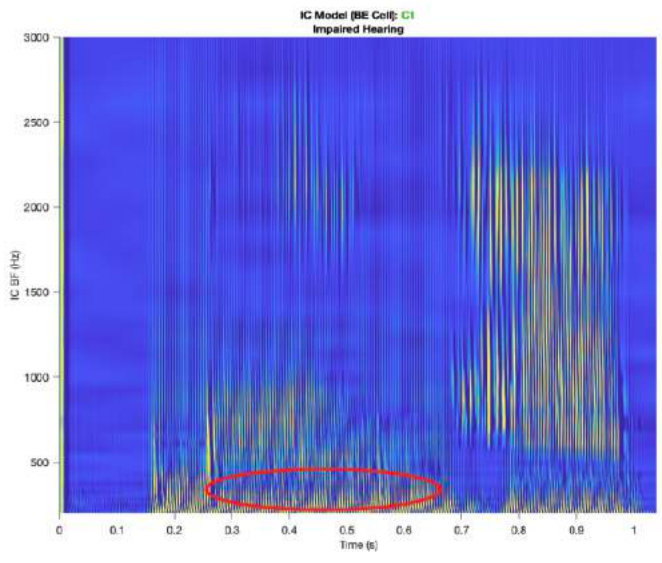

Fig. 8b) Impaired Hearing

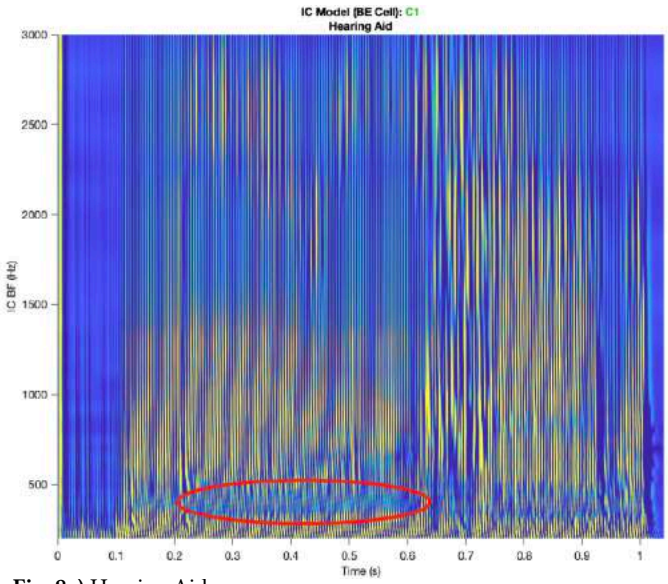

Fig. 8c) Hearing Aid

Table II: Vowel, intensity (dB), pitch (F_0), and the formants (Hz) of the words containing vowels while singing for normal hearing

Word	Intensity (dB)	Pitch (F0) (Hz)	F1 (Hz)	F2 (Hz)	F3 (Hz)
H***a***ppy	59.70	113.0	915	1731	2615
B***i***rthday	58.85	113.0	522	1840	2442
M***a***ry	63.80	96.5	613	2057	2570
L***i***ttle	64.80	96.7	551	1943	2560
L***a***mb	62.90	96.3	795	2178	3204
Tw***i***nkle	62.50	117.6	423	2215	2928
L***i***ttle	66.00	122.7	608	2058	2559
St***a***r	66.10	112.0	781	1432	2753

words containing vowels in the sentences used in speaking. The values were measured on PRAAT using the spectrogram and were compared to the dips seen in the IC model. The methods used to find the values for singing are the same as those used in speaking. The vowels measured in these words are bolded and italicized in the table below. Additionally, the intensity, pitch, and formants are measured at a single point: the vowel itself.

Figure 9 depicts the singing responses in the IC for the vowel 'a' in 'Mary' (the first second) in normal hearing, impaired hearing, and hearing aid (Ear Machine). Impaired hearing has a weaker response than the hearing aid. This is because the hearing aid amplifies the sound and thus has a higher sound level (79 dB SPL).

Speaking vs. Singing

Comparing the intensity and pitch for specific vowels in the words found in Tables I and II, singing depicted an increase in both, whereas the formants remained relatively similar to each other. Additionally, it was beneficial to compare the average IC rate in spikes per second to see the saturation in different types of hearing. To compare the IC responses accurately, the same single point of the vowel 'a' in 'Mary' was used. Figure 10 depicts these comparisons looking at the average IC rate in spikes per second.

In Figure 10, the first formant is more clearly seen in normal hearing and impaired hearing conditions. The red arrow in each plot represents the dip depicting the first formant in singing, whereas the purple arrow represents the first formant for speaking. These values correspond to the values found on PRAAT, which are seen in both Tables I and II. Additionally, speaking tended to have a higher rate. However, in the impaired ear, the dips turned into peaks. Since the impaired ear does not have saturated responses at the formant locations, it will excite slightly near a peak in the spectrum. Comparing Figure 10a with 10c, dips can be seen in 10a whereas peaks are seen in 10c at the first formant.

Discussion

For reciting in the normal hearing section (Figures 1 and 2), the vowel formants were evident in the IC model for both spoken and recited Quranic verses. Since the words were elongated in the recited version, the vowels were more evident. Reciting in the impaired ear version showed a lack of IC response at higher CFs as observed in Figures 3 and 4. Nonetheless, some vowels have still shown on the IC response, indicated by dips at their formants marked by the red ovals in

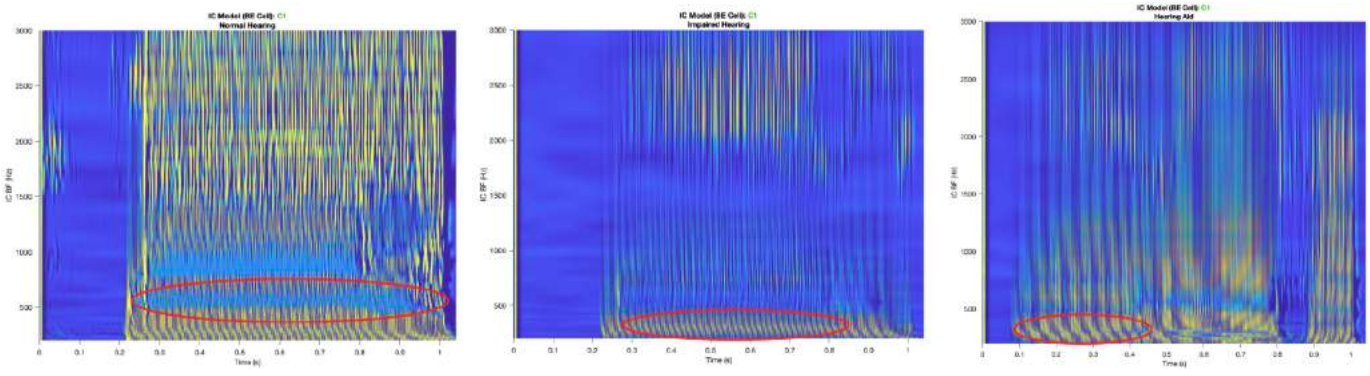

(a) **(b)** **(c)**

Fig. 9) IC Responses to singing 'Mary had a Little Lamb': (a) Normal Hearing (b) Impaired Hearing (c) Hearing Aid. The ovals represent the dips in the IC response due to the vowels in the first second to see the dip in the vowel 'a' in 'Mary.'

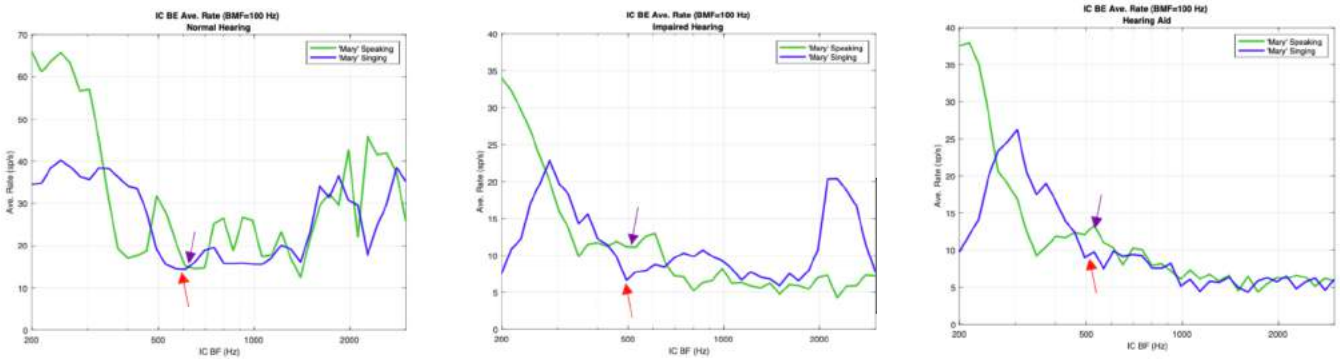

(a) **(b)** **(c)**

Fig. 10) How well the formants are encoded in the average IC Rate (spikes/sec) for speaking and singing 'Mary had a Little Lamb': (a) Normal Hearing (b) Impaired Hearing (c) Hearing Aid. This is for the first second of the sound to represent the vowel in 'Mary.'

Figures 3 and 4. For the impaired ear aided with Ear Machine, the response to reciting at higher CFs was restored, though not fully as in a healthy ear, as shown in Figures 5 and 6. This is caused by the enhancement of the higher frequency components of the sound due to the use of Ear Machine.

For the three songs spoken, strong dips can be seen on the vowel of the word 'Mary' for the healthy hearing condition (refer to Figure 8). The hearing aid IC response is much stronger than the impaired hearing as the sound is amplified, thus causing a stronger response. Additionally, 'Twinkle Twinkle Little Star' has a strong IC onset response, given that 't' is a stop constant.

However, for singing, the fundamental frequencies were much higher than in speaking. Furthermore, singing has a stronger IC response as it encompasses different pitches and more fluctuations, and the tone is steadier. Looking at 'Happy Birthday,' the 'happy' and 'birthday' are elongated during singing. Consequently, greater fluctuations are seen in both normal hearing and impaired hearing. For the hearing aid, clear dips are seen in the lower frequencies. These results are also seen for 'Twinkle Twinkle Little Star' and 'Mary had a Little Lamb.'

In Figure 10, the IC BE average rate for speaking tends to have a higher rate (spikes/second) in comparison to singing. The average rate (spikes/second) is highest in the normal hearing in comparison to impaired and hearing aid, as seen in the y-axis of Figure 10. Additionally, the first formants are well encoded in the IC rate (refer to the circle and arrows). In analyzing the spectrogram, the first formants are clearly seen where the rate first dips. However, comparing the dips and peaks due to insensitive hearing illustrates the complex effect of hearing loss on the neural responses.

Conclusion

To conclude, the results from the healthy ear showed clear dips corresponding to the formants of the vowels in speech, singing, and reciting. The impaired hearing results were promising, as the vowels' formants caused clear dips in the IC response. However, there was a lack of response in the IC due to the audiogram having higher thresholds at higher frequencies. This lack of response was restored by using the Ear Machine app as a hearing aid model. With the hearing aid model, the IC response has also shown dips at lower frequencies corresponding to the first formant.

To improve this study in the future, it would be best to test different loudness and fine-tuning values in the Ear Machine to observe and compare the different responses. Although these results give an idea of the differences between speech and singing processing early on in the processing timeline, further studies regarding the responses in subsequent parts of the brain should be carried out before revising treatment for individuals with hearing loss.

Acknowledgements

We would like to acknowledge Dr. Laurel Carney, Dr. Joyce McDonough, and The University of Rochester Biomedical Engineering, Linguistics, and Neuroscience Departments.

References

Christopher J. Plack. The Sense of Hearing. Abingdon, Oxon; New York, NY: Routledge, 2018.

Purves D, Augustine GJ, Fitzpatrick D, et al. "Integration in the Inferior Colliculus." Neuroscience 2. Sunderland, MA: Sinauer Associates, 2001.

Ziegler, Pascal, Philipp Wahl, and Peter Eberhard. "Vibration of the Basilar Membrane and Fluid Pressure Distribution in the Human Cochlea." Pamm 17, no. 1 (March 15, 2018): 229–30. https://doi.org/10.1002/pamm.201710084.

Champoux, Francois, Corinne Tremblay, Claude Mercier, Maryse Lassonde, Franco Lepore, Jean-Pierre Gagne, and Hugo Theoret. "A Role for the Inferior Colliculus in Multisensory Speech Integration." NeuroReport 17, no. 15 (October 23, 2006): 1607–10. https://doi.org/10.1097/01.wnr.0000236856.93586.94.

Pépiot, Erwan. "Processing Female and Male Voices: A Word Spotting Experiment." Perceptual and Motor Skills 117, no. 3 (December 1, 2013): 903–12. https://doi.org/10.2466/24.27.pms.117x31z7.

Fujii, Shinya, and Catherine Y. Wan. "The Role of Rhythm in Speech and Language Rehabilitation: The SEP Hypothesis." Frontiers in Human Neuroscience 8 (October 13, 2014): 77. https://doi.org/10.3389/fnhum.2014.00777.

Kim, Seung-Goo, Lepsien, Joran, Fritz, Thomas Hans, Mildner, Toralf, and Mueller, Karsten. "Dissonance encoding in human inferior colliculus covaries with individual differences in dislike of dissonant music." Scientific Reports 7, no. 1 (July 18, 2017): 5726, doi: 10.1038/s41598-017-06105-2.

Merrill, Julia, and Larrouy-Maestri, Pauline. "Vocal Features of Song and Speech: Insights from Schoenberg's Pierrot Lunaire." Frontiers in Psychology 8, (2017): 1108-1108, doi: 10.3389/fpsyg.2017.01108.

C. Laurel, Schwarz, D., Clarke, H., Doherty, K., "Enhancing Vowels: A Strategy based on Neural Fluctuations," In Prep., 2020.

EarMachine version 1.2.2, 2017. earmachine.com

Zilany, Muhammad, Bruce, Ian, and Carney, Laurel. "Updated Parameters and expanded simulation options for a model of the auditory periphery." The Journal of the Acoustical Society of America 135. no. 1 (January 2014): 283-386, doi: https://doi.org/10.1121/1.4837815

Nelson, Paul, and Carney, Laurel. "A phenomenological model of peripheral and central neural responses to amplitude-modulated tones." The Journal of the Acoustical Society of America 116. no. 4 (October 2004): 2173-2186, doi: 10.1121/1.1784442

Carney, Laurel. "Supra-Threshold Hearing and Fluctuations Profiles: Implications for Sensorineural and Hidden Hearing Loss." Journal of the Association of Research in Otolaryngology 19. no. 4 (August 2018): 331-352, doi: 10.1007/s10162-018-0669-5

Appendix

The recordings that were created for this article have been hosted and made available on Google Drive and can be found at https://drive.google.com/drive/folders/1DXfPqqoXysC-Sa8o-XL9iJDr6oRkUCdUL?usp=sharing.

A Forgotten Whaling Wife: Eunice Lawrence of Falmouth, Massachusetts

Marija Miklavčič '22, History

Advised by Dr. Richard King, *SEA Maritime History Professor*

In the 1850s, whaling was one of the most prominent industries in the United States. In the town of Falmouth, Massachusetts—the "elbow" of Cape Cod—nearly 34% of men identified themselves as either "Mariners" or "Master Mariners." This proportion increases further when taking into consideration those "involved in the ancillary seafaring trades [such] as coopers, shipwrights, sailmakers, and blacksmiths." Whaling, however, was a dangerous occupation with an average of one man dying per voyage. It also required sailors to be away from their loved ones for years at a time. In the first part of the nineteenth century, the industry began adapting to compensate for this by allowing captains to bring their wives to sea. One of the women who faced this life of isolation and danger on the open ocean was Eunice Lawrence.

In December 1853, Eunice set sail aboard the *Commodore Morris,* Her husband, Lewis Lawrence, was the captain. This whaling voyage departed from the Lawrences' hometown of Falmouth and cruised down the Eastern coasts of the Americas before it rounded the tip of South America, passing through the perilous Cape Horn. From there, they sailed into the vast Pacific Ocean. The majority of the cruise was spent in the South Pacific, hopping from island to island in search of whales, with the occasional foray northward to the equator. Two islands played a larger role in the voyage of the *Commodore Morris* than the multitude of others they visited or sailed by. The *Commodore Morris* repeatedly looped back to Moorea and Norfolk as these were the places where Eunice Lawrence was left to live among strangers, thousands of miles from home, once she gave birth to her first two sons.

Eunice's own explanations of her experiences have been lost to time. Eunice either did not keep a journal or it has been lost over the last 170 years. Similarly, there is no record of any letters written by her, describing the highs and lows of her new maritime life. As such, Eunice's story is outlined by the official record of the voyage and illuminated by the journals of other whaling wives. The official record of the voyage was called the logbook, an unimpassioned journal of sorts, detailing the weather and wind, what work was being done about the ship, and so on. It was kept by one of the mates (otherwise known as officers). The logbook also noted what ships the *Commodore Morris* met on the water and when the captain and his "Lady" went ashore. Through this logbook, Eunice's basic whereabouts and activities are known for the entirety of the voyage. Other documents—currently held by the Falmouth Public Library—include a newspaper clipping with an article written on Lewis and Eunice's fiftieth wedding anniversary, a scan of paragraph-long biographies on the Lawrence wives (Eunice included), and a document written by Eunice's son when he revisited his birthplace in the Pacific. Complementing these relatively objective sources are the journals of other whaling wives; the subjectivity helps to infer how Eunice might have truly felt about and reacted to the plethora of situations she faced.

Eunice's life before going to sea

Born in 1828 in Falmouth, Massachusetts, Eunice Freeman Davis likely knew the Lawrence family growing up. In the summer in which she was twenty-one years old, Eunice married the second youngest of the seven Lawrence siblings, Lewis. As was the whaleman tradition, both the courtship and the engagement would have been incredibly brief such that the sailor could be married before he had to go whaling again. Despite the rush, it was a match of which the Davis family likely approved. In addition to the Lawrence family being known for its piety, it was also prosperous: five of the six brothers were successful whaling captains and, once they retired from the sea, entrepreneurs. It was not long before Eunice and Lewis were separated. No more than a couple of months after their marriage, Lewis set sail on the *Commodore Morris*' maiden voyage. It was also his first trip as captain. With an absent husband and no children, Eunice's life remained virtually unchanged for the next four years. She likely even continued living with her parents. However, she had to deal with the anxious uncertainty of whether Lewis would make it home safely.

By the mid-1850s, it was relatively common for women to be on whaleships,— approximately 15% of whalers had captains' wives aboard. As such, Eunice's family was probably less concerned about scandal than the families of the early whaling wives, some of whose families disowned them. Nevertheless, the Davis family undoubtedly had their concerns. Even though Eunice would not be in a small boat battling an angry and injured whale, any maritime adventure had more than its fair share of risks: bad weather, running out of food, getting lost, and illness were only a few of the possible dreaded fates. An additional concern, however, was that Eunice may have been pregnant at their time of departure.

Eunice aboard the *Commodore Morris*

Life on a sailing vessel, even today, is extraordinarily different from life on land. Eunice went from being able to roam her town at will to being confined to three rooms and having a

limited amount of time on deck in the fresh air. She also went from having a decent variety of fresh food to living on preserved meats and vegetables and food that may have been spoiled or infested with bugs and worms. These changes would have been difficult for any of the captains' wives to navigate.

Furthermore, Eunice's pregnancy would have made her adjustment period much more uncomfortable. Not only would she likely face seasickness, and on top of that, undesirable food, but both would have also been compounded by morning sickness. Additionally, it is easier to manage seasickness from the deck, where one can combat nausea with fresh air and watch the horizon. Many of the sailors, however, found it an uncomfortable interference to have a lady on deck, and the logbook does little to suggest that the *Commodore Morris*' crew would have felt differently. Therefore, Eunice may have opted to—or felt obligated to—spend the majority of her first few months at sea suffering through the adjustment and sickness in the small, poorly ventilated cabins belowdecks.

About two weeks into the voyage, Eunice would have begun to develop her sea legs. Now, she had to figure out how to fit into the workings of the ship. All of the household duties she would have undertaken at home were the responsibilities of others on the ship. One area whaling wives most clashed with the crew was over the duty of cooking. Women were not allowed in the galley (the ship's kitchen), but there were ways around this. Eunice's sister-in-law, for example, managed to negotiate with the cook on her ship so that she was able to prepare a pie in the forward cabin that the cook would then take to the galley to bake. Trying to be helpful, Eunice may have been either setting the places for a meal or carrying food to the table when, as the logkeeper recorded, "Mrs. Lawrence broke a plate." This is an unusual comment to be in the logbook. It has nothing to do with the affairs of the ship or crew, and neither did it impact the ship's search for whales. It seems, in the overall scheme of things, irrelevant. Despite this, the logkeeper deemed it worthy to be recorded in the logbook. Perhaps the plate held part of the meal and the logkeeper was bitter over the loss, or the plate was just a plate and the logkeeper simply held a grudge against the captain's wife.

While the logkeeper never recorded another remark about Eunice's follies, the plate incident might speak to how the crew felt about having a woman on board. Many of them may have felt resentment towards her, as this was relatively common aboard whaleships. In some situations, sailors viewed their time at sea as "an escape from the company of women," and this was hampered by the presence of the captain's wife. In other situations sailors found captains' wives intrusive due to the noise of their young children or through their evangelistic efforts. Whether or not this resentment was shared by the others in the officers' quarters would have caused discomfort for Eunice. As it was, Eunice would not have been allowed to speak with most of the crew–or rather, they would not have been allowed to speak to her. In all, there were no more than a dozen of the thirty-odd people aboard whom she was allowed to interact with on a day-to-day basis during the five-year voyage. These people included the four officers, who likely had varying feelings towards Eunice, and she them; the steward and cook, with whom Eunice may have clashed over galley privileges; her husband, who as the captain was very busy; and the cabin boys, if there were any.

Luckily, there were other avenues through which Eunice could spend time with people. Although they were infrequent, meetings with other ships (gams) could even lead to years-long friendships. These gams were opportunities to exchange news, letters, gifts, and tall tales of maritime adventures. While they often lasted for only a few hours in the afternoon (as weather allowed), they were drawn out as much as possible when both ships carried women. Two ships with whom the *Commodore Morris* gammed and developed maritime friendships were the *Mohawk* of Nantucket, and the *Othello* of New Bedford. Both of these ships had whaling wives on board, and the *Mohawk* even held a family. Whenever the *Commodore Morris* met up with one of these ships, it was a multi-day affair. During a gam with the *Othello*, the Lawrences and the Beckerman family traded visits to each other's ships for four days before they needed to part ways. There were similar exchanges with the *Mohawk*. In July 1855, the *Mohawk* and the *Commodore Morris* gammed six times in a single month. Another time, the family from the *Mohawk* even stayed the night on the *Commodore Morris* before both families returned to the *Mohawk* for the rest of the day.

Even more rare than gamming with another woman, however, was when there were multiple "petticoat whalers"—whalers with women on board—in a single place. This stroke of fortune only occurred twice during Eunice's years at sea: once in a three-way gam with both the *Mohawk* and the *Potomac*, and another time with the *James Arnold* and the *Sea Gull.* Unlike gams in which just two ships and ladies were involved, these gams tended to be briefer. Whereas a gam between the *Commodore Morris* and the *Othello*, for example, lasted the better part of a week, the event between the *Commodore Morris*, the *Mohawk*, and the *Potomac* lasted a single day. Perhaps the *Potomac* and her crew were eager to return to whaling,as the *Commodore Morris* and the *Mohawk* continued their gam for another day, it is doubtful that the *Potomac* was forced away by unfavorable weather.

Other special gams were with ships from the Lawrences' home port of Falmouth or with the ships of captains Eunice and Lewis already knew. This may have happened a number of times throughout the voyage, especially in the latter part when they began running into the *Awashonks* and the *Hobomok*, both from Falmouth, Massachusetts. Whether or not they knew the captains personally, they would likely have heard of them, and there was a chance that they might be carrying letters from loved ones back home. One particular gam stands apart from all of the rest. Just a couple of months into their voyage, the *Commodore Morris* caught sight of the whaler *Anaconda*, out of New Bedford. The significance of

this ship was that the captain was family. Thomas and Mercy Lawrence were the first of the Lawrence couples to go to sea together, and they brought with them their daughter Fanny. For Eunice, pregnant with her first child and in an entirely foreign environment, it was a great relief to see her sister-in-law. Mercy, having been at sea for a couple of years already and a mother for even longer, likely had some good advice

Despite how much Eunice might have savored these opportunities to spend time with other people, the most significant experiences of the voyage would have been when she gave birth to her sons. Eunice was dropped off on Moorea in June 1855, "where she [was] to remain for our cruise" to give birth to her first son. This was only six months after the *Commodore Morris* first set sail, meaning that she could have been a couple of months pregnant at the time of departure. On the other hand, since Eunice was on Moorea for about a year, she might have been pregnant on the ship for a much shorter time before being delivered to dry land to wait out her pregnancy. Presumably, she would have remained on land for at least a few months after the birth of her child to ensure his health and to hopefully decrease any disruption a new baby might cause the runnings of the ship. In this case, she may have been further along before being dropped off on Moorea.

As soon as Eunice suspected her pregnancy, Lewis likely began making plans. How long did they have before she needed to be settled on land? Where could she go that was relatively close to the *Commodore Morris*' planned cruise track, and where she would also be safe and comfortable? Eunice was on Moorea for close to a year before the *Commodore Morris* returned for her. When Lewis dropped her off, Eunice probably moved into some rooms, either in a missionary's home or in a boarding house. While she would be surrounded by people like her–white, Christian, and perhaps even fellow whaling wives–she was still thrust into an unfamiliar setting with only strangers for company. The fear and anguish she undoubtedly felt must have been greater than any she had previously experienced. She was a young, twenty-six-year-old woman 6,500 miles from home about to give birth for the first time in a community of strangers. These uncertainties would have been compounded by concern for her husband at sea. If something happened to him, she might never return home.

Nevertheless, Eunice made it through two other pregnancies and deliveries . She gave birth to her second son on Norfolk Island in 1857 and her fourth in Honolulu in 1867, when she went to sea again some years later aboard the *Ohio*. The second time, at least, was likely easier than the first because she never went too long without seeing Lewis. In the year she was on Norfolk Island, the *Commodore Morris* returned twice before it picked her up for the return journey. Eunice's ability to form friendships while under such circumstances speaks to her fortitude and resilience. When her second son Augustus returned to his birthplace at Norfolk Island thirty years later (three visits from 1886-1888), he met people who had known his parents. Eunice only lived on Norfolk Island for a single year, and yet there were people who remembered her decades later.

Whether or not the looping of the *Commodore Morris*' cruise track was accounted for by Lewis' shore-bound boss—the "agent" of the voyage—is unclear. Even if the agent approved of this, it may have negatively affected the success of the voyage. On Lewis' first cruise as captain, he collected 1,860 barrels of sperm oil. On his cruise with Eunice, he collected only 1,098 barrels. This decrease in productivity could be the result of other factors , as the shipboard community of the *Commodore Morris* experienced its share of drama while Eunice was on Norfolk Island. Between January 1857, when Eunice was dropped off, and February 1858, when she was picked up for the trip home, two men died: the cook died of an unspecified illness while a foremast hand fell overboard and was run over by the ship. Additionally, there was a stabbing over a game of cards and the ship sprang a bad leak. It is unclear what Eunice may have heard about this from other ships coming into port at Norfolk Island while waiting for Lewis' safe return, but eventually, the ship returned for the last time and she joined it, homeward bound.

Life after the *Commodore Morris*

On October 16th, 1858, the *Commodore Morris* returned to Falmouth, Massachusetts. While most whalers turned back to the sea within a few months, Lewis remained home for a full two years. This was special for the small family as it marked the longest Lewis had been home since he first set sail at age nineteen. This period of shore-bound domesticity, however, concluded with mourning. In 1859, Eunice gave birth to her third son, Charles Grant Lawrence, and in October 1860, Lewis departed on his penultimate whaling voyage, leaving Eunice and his three sons at home in Falmouth. Six days later, baby Charles died. It is unclear if Charles even made it to a year of age. A short biography of the Lawrence wives empathizes, "What heartache for Eunice, to be home alone with two small children and to lose a baby, knowing that her husband was not likely to be home for years."

In August 1866, Eunice set sail for her second and final cruise aboard the *Ohio*, out of New Bedford. She brought both of her surviving sons and gave birth to her last child, Frederick, in Honolulu. This was the last whaling voyage Lewis took, and he never looked back. A newspaper article written in celebration of Eunice and Lewis' fiftieth anniversary wrote that Lewis "counted his REAL living as beginning when he left the sea." According to this article, Lewis also turned down $1,000 in favor of staying on land with his wife when a whaling company wanted him to return to the sea. Following his whaling career, Lewis joined the Congregational Church as a deacon and started an ice trading business. Lewis and Eunice remained in Falmouth and are buried at Oak Grove Cemetery.

Due to the purpose of the logbook and its infrequent references to Eunice, there is much that remains unknown about Eunice's experience on the *Commodore Morris*. One of the

most significant outstanding questions is whether Eunice wanted to go to sea in the first place. While some captains' wives, like Abby Jane Morrell, "abandoned patience" with being separated from their husbands and demanded to be brought along, other wives were forced into the spartan life of isolation. Others did not want to go, but did so anyway out of a sense of religious or wifely duty. Another question is the frequency of childbirth at sea versus on an island. Was Eunice's situation–being left on a conveniently located island for a full year to give birth, let alone twice–the norm for pregnant whaling wives or was it an experience unique to her? Whether or not Eunice willingly went to sea would have colored her entire experience, and her reaction to the changes she faced. What worldviews did she have going into the experience? Did any of them change based on experiences she had either at sea or on small islands that were so different from home? What stories did she tell when she returned to Falmouth?

The logbook, despite its shortcomings, provides enough of an outline of Eunice Lawrence's maritime story that it can be added to the stories of other whaling wives who lived lives of isolation and deprivation as they roamed the seas for years on end. While also adjusting to being pregnant, Eunice adapted to shipboard life, sometimes clashing with the officers and occasionally having the opportunity to gam with other whaling wives. Through gams, Eunice developed maritime friendships which lasted the full duration of her voyage, as with the family aboard the *Mohawk*. When her pregnancy demanded she leave the ship and be shore-bound on a small island in the South Pacific, she went through the trying experience only to repeat it another two times on her second cruise. In a time when very few people travelled far from home, let alone out of the Western Hemisphere, Eunice traveled tens of thousands of miles, lived on two separate islands in the South Pacific, each for a year at a time, and visited countless others from South America to New Zealand. Centuries before the globalized world, Eunice was known and loved by people on Norfolk Island and in Falmouth, Massachusetts—two communities on opposite sides of the Earth.

References

Brewster, Mary. She was a Sister Sailor: The Whaling Journals of Mary Brewster, 1845-1851. Edited by Joan Druett. Mystic, CT: Mystic Seaport Museum, Inc., 1992.

Creighton, Margaret S. Rites & Passages: The Experience of American Whaling, 1830-1870. New York City, NY: Cambridge University Press, 1995.

Druett, Joan. Petticoat Whalers: Whaling Wives at Sea, 1820-1920. Hanover, NH: University Press of New England, 1991.

"Eunice Lawrence, short bio.pdf." From the Falmouth Public Library.

Lawrence, Augustus. "Impressions of Visit to Norfolk Island." Written 23 Feb. 1907 in Falmouth, MA. In the possession of the Falmouth Public Library.

Lawrence, Mary Chipman. The Captain's Best Mate: The Journal of Mary Chipman Lawrence on the Whaler Addison, 1856-1860. Edited by Stanton Garner. Hanover, NH: University Press of New England, 1966.

"Lewis & Eunice Lawrence Anniversary001.pdf." From the Falmouth Public Library.

"Logbook of the Commodore Morris, 1849-1853." From the Falmouth Historical Society.

"Logbook of the Commodore Morris, 1853-1858." From the Falmouth Historical Society.

Malloy, Mary. "Whaling Brides and Whaling Brothers: The Lawrences of Falmouth." Falmouth, MA: The Falmouth Historical Society, 1997.

Norling, Lisa. Captain Ahab Had A Wife: New England Women and the Whalefishery, 1720-1870. Chapel Hill: University of North Carolina Press, 2000.

Whaling History: Connecting All Things Whaling. New Bedford Whaling Museum and Mystic Seaport Museum. Accessed 29 July 2020. https://whalinghistory.org/?s=AV00895.

Starbuck, Alexander. History of the American Whale Fishery, From its Earliest Inception to the Year 1896. New York City, NY: Argosy-Antiquarian, 1964.

This page left intentionally blank.


MELIORA
The
Rochester

Represent Rochester.

Join JUR.

Featured in This Issue

Investigating the Phase Behavior of Bead-Spring Polymer Blends With Molecular Dynamics Simulations
Oion Akif '21, *Chemical Engineering*

Phase diagrams of polymer mixtures are useful in a myriad of areas, including applications in industry, materials science research, as well as many other scientific applications. Use of such diagrams enable better prediction of experimental outcomes. If a particular phase is desired for a material such as a paint, coating, or ink due to its desirable properties, a phase diagram can assist in providing valuable information about the most feasible conditions it exists in, which can allow for more efficient augmentation of experiments for its creation. In this work observe the effect of changing two variables, temperature and interaction parameter between beads, of two-bead polymer systems. These two systems were seen to behave similarly to each other in terms of phases and the temperature/interaction parameter sets which resulted in them. Four different phases were identified for each system. The RDFs of each phase were inspected to investigate the spacial relationship between like and unlike beads for each phase, and how this realted to the mixing of the two polymers.

Review: Deep Brain Stimulation as Treatment for Obsessive Compulsive Disorder and Suggested Targets
Michaela Alarie '21, *Biomedical Engineering*

Mental disorders have become increasingly diagnosed worldwide. Up to 50% of all Americans will meet clinical criteria for a mental disorder within their lifetime. Despite this unnerving statistic, existing treatments for psychiatric disorders remain limited, and even treatments deemed successful by medical practitioners fail to fully rid patients of their symptoms. This review describes Obsessive Compulsive Disorder, an anxiety disorder, and investigates a relatively new approach to treating patients for whom traditional methods are not effective.

The Representation of Vowel formants in the Inferior Colliculus due to Singing, Reciting, & Speech
Akshay Sharathchandra '21, Mohammed Abumuaileq '21 & Victoria Figarola '21, *Biomedical Engineering*

Hearing is a complex process that activates several regions of the brain. Sound stimuli, including speech and music, are converted from mechanical stimuli to electrical signals through the auditory nerve pathway. This pathway stimulates the cochlear nucleus and inferior colliculus where encoding and processing occur. Speaking, singing, and chanting are identified as popular modes of communication, each of which can be characterized by different rhythms and modulations of vowels. In this investigation, the vowel formant coding of short stimuli, that includes speaking, singing, and reciting was studied across different hearing conditions: healthy, impaired, and impaired with hearing aid. The results have shown that the formants are more clearly visible in the healthy ear and are missing from the impaired ear, especially at higher frequencies. The lack of response at higher frequencies was restored by using a hearing aid.

A Forgotten Whaling Wife: Eunice Lawrence of Falmouth, Massachusetts
Marija Miklavčič '22, *History*

In the 1850s, whaling was one of the most prominent industries in the United States. In the town of Falmouth, Massachusetts—the "elbow" of Cape Cod—nearly 34% of men identified themselves as either "Mariners" or "Master Mariners." This proportion increases further when taking into consideration those "involved in the ancillary seafaring trades [such] as coopers, shipwrights, sailmakers, and blacksmiths." Whaling, however, was a dangerous occupation with an average of one man dying per voyage. It also required sailors to be away from their loved ones for years at a time. In the first part of the nineteenth century, the industry began adapting to compensate for this by allowing captains to bring their wives to sea. One of the women who faced this life of isolation and danger on the open ocean was Eunice Lawrence.

UNIVERSITY of ROCHESTER